KSME

Springer

Journal of Mechanical Science and Technology 34 (11) 2020

Original Article
DOI 10.1007/s12206-020-1006-6

Keywords:
· Cable networks
· Bending stiffness
· Free vibration characteristics
· Parameter analysis
· Vibration control

Correspondence to:
Xiaoxia Zhen
xxzhen@scut.edu.cn

Citation:
Chen, W., Zhang, Z., Zhen, X., Li, M. (2020). Effect of bending stiffness on the in-plane free vibration characteristics of a cable network. Journal of Mechanical Science and Technology 34 (11) (2020) 4439~4463.
http://doi.org/10.1007/s12206-020-1006-6

Received February 6th, 2020
Revised July 9th, 2020
Accepted August 6th, 2020

† Recommended by Editor
No-cheol Park

Effect of bending stiffness on the in-plane free vibration characteristics of a cable network

Wei Chen[1], Zhuojie Zhang[2], Xiaoxia Zhen[1] and Mingyang Li[1]

[1]School of Civil Engineering and Transportation, South China University of Technology, Guangzhou 510640, China, [2]State Key Laboratory of Mechanical Behavior and System Safety of Traffic Engineering Structures, Shijiazhuang Tiedao University, Shijiazhuang 050043, China

Abstract Stay cables of cable-stayed bridges are connected by cross-ties to form a cable network, or the slings of the same suspension points on a suspension bridge are connected by vibration absorbers to form a sling network. As a result, the cable network's in-plane free vibration characteristics are different from independent, single cables. However, stay cables or slings have certain bending stiffnesses, which directly affect the cable network's free vibration characteristics. Therefore, to clarify the real dynamic behavior of a cable network and to improve the accuracy of cable network measurements, a multi-node, cross-tied, multilayer beam analytical model that considers the bending stiffness is proposed. The system equilibrium equation is established and the free vibration frequencies and modes of the system are obtained by analytical algorithm. Then, numerical simulations and field experiments, are carried out to verify the analytical results. In addition, parameter analyses with different configurations are performed on a multilayer stay-cable network and on a double-layer sling network to study the influence of bending stiffness on the cable network's free vibration characteristics with different parameters.

1. Introduction

The stay cables of cable-stayed bridges and the slings of suspension bridges are very important structural members in long-span bridges. However, due to their small damping and high flexibility, a single cable is prone to large vibrations under the excitation of wind or traffic loads. If the cable vibrations are not eliminated or controlled effectively, they can easily cause cable fatigue, damage to the casing protection layers, and even bridge destruction [1, 2]. To control the vibration of a single cable effectively, the multiple stay cables of a cable-stayed bridge are usually connected with cross-ties, or the multiple slings of a suspension bridge are connected, at the same suspension point, with vibration absorbers to form a cable network [3], thereby forming a cooperative system that works together, as shown in Fig. 1. For this cable network, its vibration behavior is a comprehensive reflection of each cable's interactions, which is different from that of a single cable.

Usually, the cable force is obtained by testing the cable's natural vibration frequency in a real project. Among them, the cable force-frequency conversion formula, derived from string theory [4], has the widest application because this formula is simple and easy to apply. To derive a more accurate conversion relationship, many scholars have further considered the influence of factors, such as cable stiffness and sag, and have established different conversion formulas [5-7]. Generally, a cable network system needs to be simplified to resolve its internal force. In the Refs. [8-11], a sling with a vibration absorber was simplified into a single-sling model under different constraints and loads. Here Hanzheng Xu simplified the sling as a string with one end fixed and one end subjected to an elastic constraint on the vibration absorber and deduced the relation between sling tension and natural vibration frequency [8]. Further, Li simulated a sling with a vibration absorber into a two-span continuous long cable, and replaced the midspan

(a) (b)

Fig. 1. Cable network structure with intermediate node cross-ties: (a) stay cables with cross-ties; (b) slings with vibration absorbers.

support with the corresponding constrained force [9]. Gan used the finite element method to solve the sling system's natural vibration frequency with a vibration absorber [10], and Li proposed an analytical algorithm for the transverse free vibration frequency of multi-supported cable, calculating the cable frequency with intermediate supports involved [11]. To conduct the vibration analysis of a multi-support cable, Verniere equated a cable with the intermediate support to a multi-span beam under axial tensile force, and studied the dynamic characteristics of the beam with an elastic support in the middle [12]. Moreover, Xu and Lin et al. studied the dynamic characteristics of continuous multi-span beams under dynamic load, concentrated mass, torsional stiffness, linear spring, and torsional spring [13, 14]. Meanwhile, in Ref. [15], an analytical solution of the transverse natural vibration mode of a multi-span continuous long cable was obtained using the Laplace transform method. However, all these researchers [8-15] ignored the interaction between the cross-ties and the slings, and the simplified model is too simple because a suspension bridge's slings actually form a cable network system with internal node cross-ties. The system vibration is a comprehensive reflection of the interactions between cables; therefore, the cross-ties between the slings should be considered.

For cable networks, Della, and Shu et al. obtained an analytical solution for the natural vibration frequency of the local layered beam by establishing the vibration equation of the element in sections [16, 17]. Caracoglia conducted a preliminary analysis of the free vibration characteristics of double-layer and multilayer cable networks connected by cross-ties, verifying this analysis with the Fred Hartman Bridge [18, 19]. Ahmad further studied the free vibration characteristics of a cable network connected by cross-ties and proposed two indicators, using the degree of mode localization and local mode clusters, to evaluate the quality of the local modes [20, 21]. In addition, Ahmad also analyzed the free vibration characteristics of a hybrid network system with external damping [22]. Yamaguchi conducted experiments on a double-layer cable network and concluded that the modal damping increased significantly when flexible cross-ties were used, while target cable stiffness could be improved when rigid cross-ties were used [23]. Zhou studied the free vibration characteristics of two cables with dampers or cross-ties, analyzed the impact of the dampers on the cables' vibration reduction [24-26], and proposed a new index to measure the degree of mode localization [27]. In addition, Zhou derived an analytical formula of the in-plane vibration equation that considered the cable sag [28]. In the Refs. [29-31], the cable-spring-damper system model was applied to the analysis of the vibrations reduction mechanism for cross-tie of cable-stayed bridges. The Ref. [32] analyzed the mechanisms of vibration reduction from cross-ties and discussed the design of cross-ties based on the second bridge of the Yangtze river in Nanjing. The Ref. [33] determined the slings' dynamic characteristics and the separator's vibration reduction scheme by means of the environmental excitation method, conducting a comparative study on the separators' vibration reduction effect. To solve the problem of wind-induced vibration of straddle slings for suspension bridges, Lei proposed a vibration reduction method involving a separator combined with a cable-end damper [34]. However, the Refs. [16-34] did not consider the impact of the cable's bending stiffness, and the natural vibration frequency of the cable that was calculated from the theoretical formula was less than the actual value, resulting in differences from the actual situation.

The above literature shows that previous research on cable networks has a too simple simplified model or has not considered the influence of the cable bending stiffness. But the short cable or sling has a great bending stiffness in a real project that cannot be ignored. In the previous research on the free vibration characteristics of a coupled cable network, the bending stiffness of the cable was ignored, resulting in the free vibration frequency of the network calculated using the theoretical formula being less than the true value, while the mode shape was not completely analogous, which resulted in a discrepancy between the calculations and the actual situation. Therefore, it is necessary to consider the bending stiffness of the cable when examining the actual cable network, to ensure that the system frequency and the mode shape obtained using the theoretical formula are closer to the reality. This will provide more accurate data for the analysis of the cable network vibration reduction mechanism, which will be highly valuable in terms of engineering applications.

To study the bending stiffness' influence on a cable network's in-plane free vibration characteristics, this paper uses the multi-node, cross-ties, multilayer beam element model considering the bending stiffness as the research object to derive the vibration equation for the cable network's cross-tie vibrations. After the vibration frequency and mode are solved, the calculation results are verified by numerical simulation and experimental methods. Parameter analyses with different configurations are performed on a multilayer stay-cable network, whose lengths are unequal, and on a double-layer sling network, whose lengths are equal. The analyses include cross-tie stiffness, cross-tie position, number of cross-ties, number of stay cables of the stay-cable network and slings lengths, vibration absorber stiffness, vibration absorber position, and the number of vibration absorbers in the sling network to study the

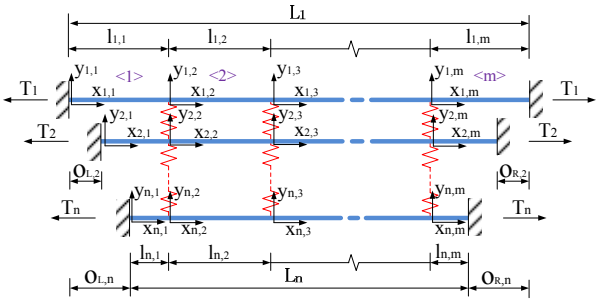

Fig. 2. Analytical schematic of the cable network.

influence of bending stiffness on cable networks' free vibration characteristics with different parameters.

2. The vibration equation of a cable network and its solution

2.1 Analysis model of a cable network

Fig. 2 shows a cable network consisting of *n* independent anchored horizontal cables which are of unequal length. The longest cable length is L_1 and the other cable lengths are L_2 to L_n in turn; the cable forces are T_1 to T_n. The two ends of the cable are solid joints. The cables are connected by vertical cross-links with a certain stiffness. The cross-links divide each cable into *m* subsystems and the length of each subsystem is l_{ij} (*i* is the cable number and *j* is the subsystem number); the left end of each subsystem is used as the origin to establish the coordinate system.

2.2 Derivation of characteristic equations

While ignoring effects of the axial forces increase and damping, and considering the cable's bending stiffness, the differential equation for transverse vibration of a single cable under tension is [35]:

$$EI\frac{\partial^4 v(x,t)}{\partial x^4}-T\frac{\partial^2 v(x,t)}{\partial x^2}+m\frac{\partial^2 v(x,t)}{\partial t^2}=0. \tag{1}$$

In Eq. (1), *v(x,t)* is the cable's transverse displacement; *x* is the coordinate along the cable axis; *t* is the vibration time; *E* is the cable's elastic modulus; *I* is the moment of inertia of the cable's cross section to the central spindle; *T* is the cable tension; and *m* is the cable's mass per unit length.

Eq. (1) can be solved by the method of separating variables, and the form of solution to the equation is

$$v(x,t)=\varphi(x)q(t) \tag{2}$$

where *φ(x)* is a function of *x* and *q(t)* is a function of *t*. Substituting Eq. (2) into Eq. (1) and dividing both sides by *mφ(x)q(t)*, we obtain

$$\frac{EI}{m}\frac{\varphi^{IV}(x)}{\varphi(x)}-\frac{T}{m}\frac{\varphi''(x)}{\varphi(x)}=-\frac{\ddot{q}(t)}{q(t)}=\omega^2. \tag{3}$$

Eq. (3) can be transformed into the following two equations after separation of variables is performed:

$$\varphi^{IV}(x)-\frac{T}{EI}\varphi''(x)-\frac{m\omega^2}{EI}\varphi(x)=0 \tag{4}$$

$$\ddot{q}(t)+\omega^2 q(t)=0. \tag{5}$$

Eq. (4) is a fourth-order homogeneous linear ordinary differential equation, and its solution is

$$\varphi(x)=A\cos(\alpha x)+B\sin(\alpha x)+C\cosh(\beta x)+D\sinh(\beta x). \tag{6}$$

Among them

$$\alpha=\sqrt{\sqrt{\left(\frac{T}{2EI}\right)^2+\omega^2\frac{m}{EI}}-\frac{T}{2EI}} \tag{7}$$

$$\beta=\sqrt{\sqrt{\left(\frac{T}{2EI}\right)^2+\omega^2\frac{m}{EI}}+\frac{T}{2EI}}. \tag{8}$$

The solution of Eq. (5) is

$$q(t)=E\cos(\omega t)+F\sin(\omega t) \tag{9}$$

Let $\tilde{x}=\frac{x}{L}$, $\tilde{\alpha}=\alpha L$, $\tilde{\beta}=\beta L$, $\tilde{\omega}=\omega\frac{L^2}{\sqrt{EI/m}}$, $\xi=L\sqrt{T/EI}$, $\tilde{\varphi}=\frac{\varphi}{L}$, $\tilde{t}=t\frac{\sqrt{EI/m}}{L^2}$, $\tilde{q}=q$.

By making Eq. (6) dimensionless, we get

$$\tilde{\varphi}(\tilde{x})=\tilde{A}\cos(\tilde{\alpha}\tilde{x})+\tilde{B}\sin(\tilde{\alpha}\tilde{x})+\tilde{C}\cosh(\tilde{\beta}\tilde{x})+\tilde{D}\sinh(\tilde{\beta}\tilde{x}) \tag{10}$$

Among them

$$\tilde{\alpha}=\sqrt{\sqrt{\left(\frac{\xi^2}{2}\right)^2+\tilde{\omega}^2}-\frac{\xi^2}{2}} \tag{11}$$

$$\tilde{\beta}=\sqrt{\sqrt{\left(\frac{\xi^2}{2}\right)^2+\tilde{\omega}^2}+\frac{\xi^2}{2}}. \tag{12}$$

By making Eq. (9) dimensionless, we get

$$\tilde{q}(\tilde{t})=\tilde{E}\cos(\tilde{\omega}\tilde{t})+\tilde{F}\sin(\tilde{\omega}\tilde{t}). \tag{13}$$

Therefore,

$$\tilde{v}(\tilde{x},\tilde{t})=\tilde{\varphi}(\tilde{x})\tilde{q}(\tilde{t}). \tag{14}$$

For the cable network, the solution of the vibration equation of each cable subsystem is as follows:

$$\begin{aligned}\tilde{v}_i^{<j>}(\tilde{x}_{ij},\tilde{t})&=\tilde{\varphi}_i^{<j>}(\tilde{x}_{ij})\tilde{q}_i^{<j>}(\tilde{t})=\left[\tilde{A}_i^{<j>}\cos(\tilde{\alpha}_i\tilde{x}_{ij})\right.\\&\left.+\tilde{B}_i^{<j>}\sin(\tilde{\alpha}_i\tilde{x}_{ij})+\tilde{C}_i^{<j>}\cosh(\tilde{\beta}_i\tilde{x}_{ij})+\tilde{D}_i^{<j>}\sinh(\tilde{\beta}_i\tilde{x}_{ij})\right]\\&\times\left[\tilde{E}_i^{<j>}\cos(\tilde{\omega}_i^{<j>}\tilde{t})+\tilde{F}_i^{<j>}\sin(\tilde{\omega}_i^{<j>}\tilde{t})\right].\end{aligned} \tag{15}$$

In the equation, *i* represents the cable number and ranges from 1 to *n* and *j* represents the subsystem number and ranges from 1 to *m*.

Since the cables form a system through their cross-links, the vibration frequency of each cable is equal, that is

$$\omega_i^{<j>}=\omega. \tag{16}$$

Therefore, it is only necessary to solve the modal equation of each cable, then

$$\begin{aligned}\tilde{\varphi}_i^{<j>}(\tilde{x}_j)&=\tilde{A}_i^{<j>}\cos(\tilde{\alpha}_i\tilde{x}_{ij})+\tilde{B}_i^{<j>}\sin(\tilde{\alpha}_i\tilde{x}_{ij})\\&+\tilde{C}_i^{<j>}\cosh(\tilde{\beta}_i\tilde{x}_{ij})+\tilde{D}_i^{<j>}\sinh(\tilde{\beta}_i\tilde{x}_{ij}).\end{aligned} \tag{17}$$

2.3 Solving the characteristic equation

For the cable network shown in Fig. 2, Eq. (17) is a simultaneous equation system, with 4 *nm* undetermined coefficients, and its solution can be determined by the boundary conditions, continuity requirements, and the vertical force balance requirements.

(1) Boundary conditions

Since the two ends of the cable are solid joints, the displacement and slope at the cable end are both zero, that is

$$\begin{cases}\tilde{\varphi}_i^{<1>}(0)=\tilde{\varphi}_i^{<m>}(\tilde{l}_{im})=0\\ \tilde{\varphi}'^{<1>}_i(0)=\tilde{\varphi}'^{<m>}_i(\tilde{l}_{im})=0.\end{cases} \tag{18}$$

There are 4*n* equations.

(2) Continuity requirement

The displacements, slopes, and bending moments of the same cable at the cross-ties locations are equal, that is

$$\begin{cases}\tilde{\varphi}_i^{<s>}(\tilde{l}_{is})=\tilde{\varphi}_i^{<s+1>}(0)\\ \tilde{\varphi}'^{<s>}_i(\tilde{l}_{is})=\tilde{\varphi}'^{<s+1>}_i(0)\\ \tilde{\varphi}''^{<s>}_i(\tilde{l}_{is})=\tilde{\varphi}''^{<s+1>}_i(0)\end{cases}\quad(s=1,2...m-1). \tag{19}$$

There are 3*n(m*−1*)* equations.

(3) Vertical force balance requirements

The external force of the cable at the cross-tie locations is balanced with the shear force, that is

$$\begin{cases}\frac{E_1I_1}{L_1^2}\left(\tilde{\varphi}'''^{<s>}_1(\tilde{l}_{1s})-\tilde{\varphi}'''^{<s+1>}_1(0)\right)=k\left(\tilde{\varphi}_1^{<s+1>}(0)L_1-\tilde{\varphi}_2^{<s+1>}(0)L_2\right)\\ \frac{E_rI_r}{L_r^2}\left(\tilde{\varphi}'''^{<s>}_r(\tilde{l}_{rs})-\tilde{\varphi}'''^{<s+1>}_r(0)\right)=-k\left(\tilde{\varphi}_{r-1}^{<s+1>}(0)L_{r-1}-\tilde{\varphi}_r^{<s+1>}(0)L_r\right)\\ \qquad\qquad+k\left(\tilde{\varphi}_r^{<s+1>}(0)L_r-\tilde{\varphi}_{r+1}^{<s+1>}(0)L_{r+1}\right)\\ \frac{E_nI_n}{L_n^2}\left(\tilde{\varphi}'''^{<s>}_n(\tilde{l}_{ns})-\tilde{\varphi}'''^{<s+1>}_n(0)\right)=-k\left(\tilde{\varphi}_{n-1}^{<s+1>}(0)L_{n-1}-\tilde{\varphi}_n^{<s+1>}(0)L_n\right)\end{cases}$$

($r=2,3...n-1$; $s=1,2...m-1$; k is the spring stiffness). (20)

There are *n(m*–1*)* equations.

(4) 4 *nm* equations can be obtained from the above, and the above equation is written as a matrix:

$$\mathbf{KX}=\mathbf{0}. \tag{21}$$

$\mathbf{K}$ is a 4 *nm*×4 *nm* coefficient matrix and $\mathbf{X}$ is a 4 *nm*×1 column vector with undetermined coefficients. Among them

$$\begin{aligned}\mathbf{X}=\{&\tilde{A}_1^{<1>},\tilde{B}_1^{<1>},\tilde{C}_1^{<1>},\tilde{D}_1^{<1>}...\tilde{A}_1^{<m>},\tilde{B}_1^{<m>},\tilde{C}_1^{<m>},\tilde{D}_1^{<m>}...\tilde{A}_n^{<1>},\tilde{B}_n^{<1>},\\&\tilde{C}_n^{<1>},\tilde{D}_n^{<1>}...\tilde{A}_n^{<m>},\tilde{B}_n^{<m>},\tilde{C}_n^{<m>},\tilde{D}_n^{<m>}\}^T.\end{aligned}$$

If there is a solution to Eq. (21), then the determinant of the coefficient matrix is zero, and the characteristic equation of the system is

$$\det(\mathbf{K})=0. \tag{22}$$

Since there is only one unknown parameter $\tilde{\omega}$ in Eq. (22), it can be obtained by Mathematica. After $\tilde{\omega}$ is obtained, the cable network's free vibration frequency *f* can be calculated based on $\omega=\tilde{\omega}\frac{\sqrt{EI/m}}{L^2}$ and $f=\frac{\omega}{2\pi}$. In addition, by substituting $\tilde{\omega}$ into the equation $\mathbf{KX}=\mathbf{0}$, the coefficient column vector $\mathbf{X}$ can be obtained. Then, the vibration mode of each cable can be obtained by substituting $\mathbf{X}$ back into Eq. (17).

If the length of two cables of equal length is *L*, the two ends of each cable are solid joints, and they are connected through a cross-link with a stiffness of *k* in the midspan, we can obtain the analytical expression of the characteristic equation as follows:

$$\begin{aligned}&16EI\tilde{\alpha}\tilde{\beta}\left(\tilde{\alpha}^2+\tilde{\beta}^2\right)^3\left(\tilde{\beta}\cosh(\tilde{\beta}/2)\sin(\tilde{\alpha}/2)-\tilde{\alpha}\cos(\tilde{\alpha}/2)\sinh(\tilde{\beta}/2)\right)^2\\&\left(\tilde{\alpha}\cosh(\tilde{\beta}/2)\sin(\tilde{\alpha}/2)+\tilde{\beta}\cos(\tilde{\alpha}/2)\sinh(\tilde{\beta}/2)\right)\\&\left(2\tilde{\alpha}\tilde{\beta}kL^3+\tilde{\alpha}\tilde{\beta}\cosh(\tilde{\beta}/2)\left(-2kL^3\cos(\tilde{\alpha}/2)+EI\tilde{\alpha}\left(\tilde{\alpha}^2+\tilde{\beta}^2\right)\sin(\tilde{\alpha}/2)\right)+\right.\\&\left.\sinh(\tilde{\beta}/2)\left(EI\tilde{\alpha}\tilde{\beta}^2\left(\tilde{\alpha}^2+\tilde{\beta}^2\right)\cos(\tilde{\alpha}/2)+kL^3\left(-\tilde{\alpha}^2+\tilde{\beta}^2\right)\sin(\tilde{\alpha}/2)\right)\right).\end{aligned} \tag{23}$$

If the stiffness of the cross-link is infinite, we can obtain the analytical expression of the characteristic equation as follows:

$$4\tilde{\alpha}\tilde{\beta}\left(\tilde{\alpha}^2+\tilde{\beta}^2\right)^3\left(\tilde{\beta}\cosh\left(\tilde{\beta}/2\right)\sin\left(\tilde{\alpha}/2\right)-\tilde{\alpha}\cos\left(\tilde{\alpha}/2\right)\sinh\left(\tilde{\beta}/2\right)\right)^2$$
$$\left(8\tilde{\alpha}^2\tilde{\beta}\cosh\left(\tilde{\beta}/2\right)\sin\left(\tilde{\alpha}/2\right)-\right.$$
$$\tilde{\beta}\left(\tilde{\alpha}^2+\tilde{\beta}^2+\left(3\tilde{\alpha}^2-\tilde{\beta}^2\right)\cosh\left(\tilde{\beta}\right)\right)\sin\left(\tilde{\alpha}\right)+8\tilde{\alpha}\tilde{\beta}^2\cos\left(\tilde{\alpha}/2\right)\sinh\left(\tilde{\beta}/2\right)-$$
$$\tilde{\alpha}\left(\tilde{\alpha}^2+\tilde{\beta}^2\right)\sinh\left(\tilde{\beta}\right)+\tilde{\alpha}\left(\tilde{\alpha}^2-3\tilde{\beta}^2\right)\cos\left(\tilde{\alpha}\right)\sinh\left(\tilde{\beta}\right). \quad (24)$$

2.4 The characteristic equation without considering the cable's bending stiffness

For the cable network system shown in Fig. 2, when the effect of bending stiffness is ignored, the differential equation for the transverse vibration of a single cable under tension will be as follows:

$$m\frac{\partial^2 v(x,t)}{\partial t^2}-T\frac{\partial^2 v(x,t)}{\partial x^2}=0. \quad (25)$$

Eq. (25) can be solved using the method of separating variables, to obtain the following:

$$T\varphi''(x)+m\omega^2\varphi(x)=0. \quad (26)$$

Eq. (26) is a second-order homogeneous linear ordinary differential equation, and its solution is as follows:

$$\varphi(x)=A\cos(\gamma x)+B\sin(\gamma x). \quad (27)$$

Among them

$$\gamma=\sqrt{\frac{m\omega^2}{T}} \quad (28)$$

let $\tilde{x}=\frac{x}{L}$, $\tilde{\gamma}=\gamma L$, $\tilde{\varphi}=\frac{\varphi}{L}$, $\tilde{\omega}=\frac{\omega}{\omega_1}$, $\omega_1=\sqrt{\frac{T_1}{m_1L^2}}$, T_1, and m_1 be the cable force and the linear density of cable 1.

By making Eq. (27) dimensionless, we obtain,

$$\tilde{\varphi}(\tilde{x})=\tilde{A}\cos(\tilde{\gamma}\tilde{x})+\tilde{B}\sin(\tilde{\gamma}\tilde{x}). \quad (29)$$

Among them

$$\tilde{\gamma}=\sqrt{\frac{m\omega^2L^2}{T}}. \quad (30)$$

Similarly, we can obtain the vibration equation of each cable without considering the cable's bending stiffness:

$$\tilde{\varphi}_i^{<j>}\left(\tilde{x}_j\right)=\tilde{A}_i^{<j>}\cos\left(\tilde{\gamma}_i\tilde{x}_{ij}\right)+\tilde{B}_i^{<j>}\sin\left(\tilde{\gamma}_i\tilde{x}_{ij}\right). \quad (31)$$

Eq. (31) is a simultaneous equation system, with 2 *nm* undetermined coefficients, and its solution can be determined according to the boundary conditions, continuity requirements, and the vertical force balance requirements.

(1) Boundary conditions

As the two ends of the cable are solid joints, the displacement at the cable end is zero, that is,

$$\tilde{\varphi}_i^{<1>}(0)=\tilde{\varphi}_i^{<m>}\left(\tilde{l}_{im}\right)=0. \quad (32)$$

There are 2*n* equations.

(2) Continuity requirement 1

The displacements of the same cable at the cross-tie locations are equal, that is,

$$\tilde{\varphi}_i^{<s>}\left(\tilde{l}_{is}\right)=\tilde{\varphi}_i^{<s+1>}(0)\quad\left(s=1,\ 2...m-1\right). \quad (33)$$

There are *n(m*−1*)* equations.

(3) Continuity requirement 2

The displacement of the adjacent cable at the cross-tie locations is

$$\left(\tilde{\varphi}_r^{<s+1>}(0)-\tilde{\varphi}_{r+1}^{<s+1>}(0)\right)=\sum_{p=1}^{r}\left[\frac{T_p}{k}\left(\tilde{\varphi}_p'^{<s>}\left(\tilde{l}_{ps}\right)-\tilde{\varphi}_p'^{<s+1>}(0)\right)\right]$$
$$\left(r=1,\ 2...n-1;\ s=1,\ 2...m-1\right). \quad (34)$$

If the stiffness of the cross-ties is infinite, Eq. (34) becomes

$$\tilde{\varphi}_r^{<s+1>}(0)=\tilde{\varphi}_{r+1}^{<s+1>}(0). \quad (35)$$

There are *(n*−1*)(m*−1*)* equations.

(4) Vertical force balance requirements

The vertical force component of the cable at the cross-tie locations is balanced, that is,

$$\sum_{i=1}^{n}T_i\tilde{\varphi}_i'^{<s>}\left(\tilde{l}_{is}\right)=\sum_{i=1}^{n}T_i\tilde{\varphi}_i'^{<s+1>}(0)$$
$$\left(r=1,\ 2...n-1;\ s=1,\ 2...m-1\right). \quad (36)$$

There are *(m*−1*)* equations.

2 *nm* equations can be obtained from the above, and the above equation is then written as a matrix:

$$\mathbf{KX}=\mathbf{0}. \quad (37)$$

$\mathbf{K}$ is a 2 *nm*×2 *nm* coefficient matrix and $\mathbf{X}$ is a 2 *nm*×1 column vector with undetermined coefficients. Among them,

$$\mathbf{X}=\left\{\tilde{A}_1^{<1>},\tilde{B}_1^{<1>}...\tilde{A}_1^{<m>},\tilde{B}_1^{<m>}...\tilde{A}_n^{<1>},\tilde{B}_n^{<1>}...\tilde{A}_n^{<m>},\tilde{B}_n^{<m>}\right\}^T.$$

If there is a solution to Eq. (37), then the determinant of the coefficient matrix is zero; the characteristic equation of the system is thus

$$\det(\mathbf{K}) = 0 . \tag{38}$$

As there is only one unknown parameter ω in Eq. (38), it can be obtained using Mathematica. Once ω has been obtained, the cable network's free vibration frequency f without considering the cable's bending stiffness can be calculated using $f = \frac{\omega}{2\pi}$. In addition, by substituting ω into the equation $\mathbf{KX} = \mathbf{0}$, the coefficient column vector $\mathbf{X}$ can be obtained. Then, the vibration mode of each cable can be obtained by substituting $\mathbf{X}$ back into Eq. (31).

3. Formula verification

To verify the analytical formula's accuracy, which involves calculating the natural frequency and mode of the cable network while considering the cable's bending stiffness proposed in this paper, a model with four cables and three cross-links was established. After the natural frequency is calculated, using the analytical method in this paper, numerical simulations using the finite element software ANSYS and field experiments are performed to verify the analytical results.

3.1 Analytical algorithm

As shown in Fig. 3, a cable network is defined, consisting of four independently anchored cables whose ends are solid joints. The length L of each cable is 3.37 m. The cable is connected by three cross-links of a certain stiffness at distances of 1/10 L, 1/2 L and 9/10 L from the left end of the cable, and the cable is divided into four parts, e.g., l_1 = 0.337 m, l_2 = 1.348 m, l_3 = 1.348 m and l_4 = 0.337 m. The cross-link stiffnesses here are $k_1 = 10^7$ N/m, which is close to a rigid connection, and $k_2 = 10^4$ N/m, which is close to a flexible connection. To work with more realistic conditions, let the cable tension have a variation of 10 %; that is, the cable tensions are T_1 = 31500 N, T_2 = 30750 N, T_3 = 29250 N, and T_4 = 28500 N.

The cable parameters are shown in Table 1.

According to the above, the conditions of the cable network with four cables and three cross-links are as follows:

$$\begin{cases} \tilde{\varphi}_i^{<1>}(0) = \tilde{\varphi}_i^{<4>}\left(\tilde{l}_{i4}\right) = 0 \\ \tilde{\varphi}'^{<1>}_i(0) = \tilde{\varphi}'^{<4>}_i\left(\tilde{l}_{i4}\right) = 0 \end{cases} \quad (i = 1, 2, 3, 4)$$

$$\begin{cases} \tilde{\varphi}_i^{<s>}\left(\tilde{l}_{is}\right) = \tilde{\varphi}_i^{<s+1>}(0) \\ \tilde{\varphi}'^{<s>}_i\left(\tilde{l}_{is}\right) = \tilde{\varphi}'^{<s+1>}_i(0) \\ \tilde{\varphi}''^{<s>}_i\left(\tilde{l}_{is}\right) = \tilde{\varphi}''^{<s+1>}_i(0) \end{cases} \quad (i = 1, 2, 3, 4;\ s = 1, 2, 3)$$

Table 1. Cable parameters of cable network with four cables and three cross-links.

Cross-sectional area (m^2)	Inertia moment (m^4)	Elastic modulus (Pa)	Linear density (kg/m)
1.39×10^{-4}	1.536×10^{-9}	1.95×10^{11}	1.12

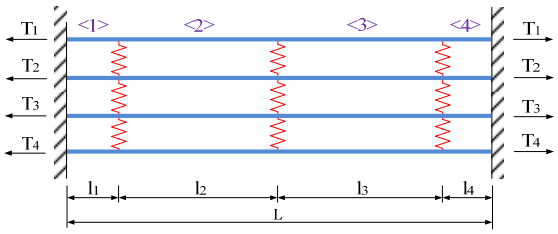

Fig. 3. Cable network with four cables and three cross-links.

$$\begin{cases} \dfrac{EI}{L^2}\left(\tilde{\varphi}'''^{<s>}_1\left(\tilde{l}_{1s}\right) - \tilde{\varphi}'''^{<s+1>}_1(0)\right) = k\left(\tilde{\varphi}_1^{<s+1>}(0)L - \tilde{\varphi}_2^{<s+1>}(0)L\right) \\ \dfrac{EI}{L^2}\left(\tilde{\varphi}'''^{<s>}_r\left(\tilde{l}_{rs}\right) - \tilde{\varphi}'''^{<s+1>}_r(0)\right) = -k\left(\tilde{\varphi}_{r-1}^{<s+1>}(0)L - \tilde{\varphi}_r^{<s+1>}(0)L\right) \\ \qquad\qquad +k\left(\tilde{\varphi}_r^{<s+1>}(0)L - \tilde{\varphi}_{r+1}^{<s+1>}(0)L\right) \\ \dfrac{EI}{L^2}\left(\tilde{\varphi}'''^{<s>}_n\left(\tilde{l}_{ns}\right) - \tilde{\varphi}'''^{<s+1>}_n(0)\right) = -k\left(\tilde{\varphi}_{n-1}^{<s+1>}(0)L - \tilde{\varphi}_n^{<s+1>}(0)L\right) \end{cases}$$

($r = 2, 3$; $s = 1, 2, 3$; k is the stiffness of cross-links).

We write the above equation as a matrix:

$$\mathbf{K}_1\mathbf{X}_1 = \mathbf{0} .$$

$\mathbf{K}_1$ is the coefficient matrix with a dimension of 64×64. If $\det(\boldsymbol{K}_1) = 0$, we can calculate the first 10 natural frequencies of a system with four cables and three cross-links using Mathematica when $k_1 = 10^7$ N/m and $k_2 = 10^4$ N/m, as f_{s1} shown in Table 2.

In addition, the first 10 natural frequencies of a system with four cables and three cross-links, without considering the cable's bending stiffness, are compared. When the stiffness of the cross-links is $k_1 = 10^7$ N/m, the fundamental frequency of the system, with four cables and three cross-links, while considering the cable's bending stiffness, is 25.92 Hz; the fundamental frequency, while not considering the cable's bending stiffness, is 24.28 Hz, thus showing a difference of 6.33 %. The maximum deviation of the first 10 natural frequencies is 13.38 %. When the stiffness of cross-link is $k_2 = 10^4$ N/m, the fundamental frequency of the system, with four cables and three cross-links, while considering the cable's bending stiffness, is 25.81 Hz; the fundamental frequency, while not considering the cable's bending stiffness, is 24.17 Hz, thus showing a difference of 6.35 %. The maximum deviation of the first 10 natural frequencies is 9.47 %.

The first 10 modes of the system with four cables and three cross-links while considering the cable's bending stiffness are shown in Fig. 4. Due to the effect of the cross-links, the local

Table 2. Comparison of the natural frequencies of a system with four cables and three cross-links.

Order	$k_1 = 10^7$ N/m					$k_2 = 10^4$ N/m				
	Analytical algorithm f_{S1}	Finite element method f_{S2}	Relative error s_1	Experimental method f_{S3}	Relative error s_2	Analytical algorithm f_{S1}	Finite element method f_{S2}	Relative error s_1	Experimental method f_{S3}	Relative error s_2
1	25.92	25.92	0.00 %	26.00	0.31 %	25.81	25.80	-0.04 %	25.02	-3.06 %
2	52.46	52.45	-0.02 %	53.59	2.15 %	27.72	27.72	0.00 %	27.34	-1.37 %
3	63.92	63.89	-0.05 %	65.92	3.13 %	31.16	31.16	0.00 %	31.01	-0.48 %
4	64.99	64.97	-0.03 %	68.12	4.82 %	34.13	34.13	0.00 %	34.42	0.85 %
5	66.21	66.20	-0.02 %	69.34	4.73 %	51.65	51.63	-0.04 %	51.39	-0.50 %
6	68.92	68.89	-0.04 %	70.80	2.73 %	52.96	52.95	-0.02 %	52.73	-0.43 %
7	69.96	69.93	-0.04 %	71.90	2.77 %	53.83	53.83	0.00 %	53.47	-0.67 %
8	71.37	71.35	-0.03 %	74.10	3.83 %	54.76	54.76	0.00 %	54.81	0.09 %
9	80.44	80.42	-0.02 %	78.98	-1.82 %	79.38	79.36	-0.03 %	76.54	-3.58 %
10	110.15	110.11	-0.04 %	108.15	-1.82 %	81.98	81.96	-0.02 %	78.74	-3.95 %

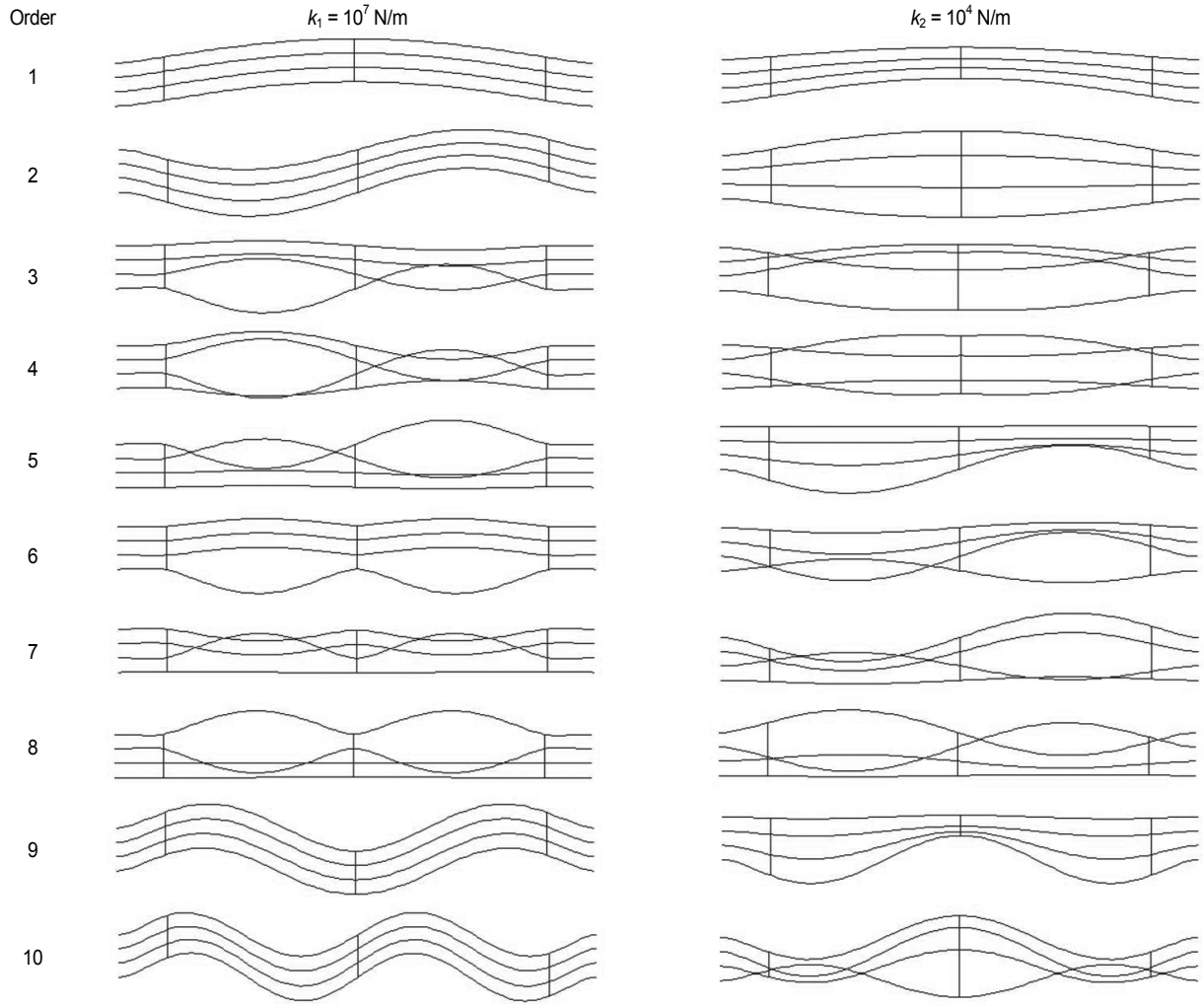

Fig. 4. First 10 modes of the system with four cables and three cross-links.

vibration frequencies appear between the global vibration frequencies. For example, the 1st, 2nd, 9th, and 10th orders are the global vibration modes, and the 3rd, 4th, 5th, 6th, 7th, and 8th orders are the local vibration modes when the stiffness of the cross-links is $k_1 = 10^7$ N/m. The 1st, 5nd, and 9th orders are the global vibration modes, and the 2nd, 3rd, 4th, 6th, 7th, 8th, and 10th orders are the local vibration modes, when the stiffness of the cross-links is $k_1 = 10^4$ N/m, for which the global vibrations are not obvious because the stiffness of the flexible cross-links is small.

3.2 Finite element method

To verify the theoretical derivation, we established a model using ANASY finite element software that incorporated four cables and three cross-links, in which the stiffness of the cable was considered. The cable was simulated using a BEAM188 element [36], and the element parameters were set according to the cable parameters listed in Table 1. The cable tension was applied as a pre-tensioning force [37], with the tensions for each cable set as follows: $T_1 = 31500$ N, $T_2 = 30750$ N, $T_3 = 29250$ N, and $T_4 = 28500$ N. The two ends of the cable were solid joints. The cables were connected at 1/10 *L*, 1/2 *L* and 9/10 *L* with the cross-links, and the cross-links were simulated using COMBIN14 elements with a stiffness of $k_1 = 10^7$ N/m and $k_2 = 10^4$ N/m. Following the modal analysis, the first 10 natural frequencies of the finite element model were obtained as the f_{s2} values given in Table 2. These frequencies as calculated by the ANSYS software were very close to the equivalent frequencies calculated using the analytical algorithm in this work. The maximum error was only −0.05 %, meaning that the two methods essentially produced the same results.

3.3 Experimental method

The theory was also verified through field experiments. In terms of the engineering properties of the test cables, they were steel strands with a cross-sectional area of 1.39×10^{-4} m^2. Here, the cross-sectional area (A), bending stiffness (EI), and linear density (m) were consistent with those listed in Table 1.

Fig. 5 presents a panorama of the field experiments. Four steel strands with a specific tensile force were anchored on a self-made force frame. The ends of the cables can be regarded as solid joints owing to the action of the anchor head. After the tensile forces of the steel strands were applied through a jack with an oil pressure gauge, the tension values were finely adjusted by rotating the nut on the right side of the steel strand until the tensile force reached the desired value. The tension is measured by the pressure sensor on the left side of the steel strand and is read by a static strain testing system connected to the pressure sensor. The pressure sensor is shown in Fig. 6(a). The relationship between the tensile value of the pressure sensor and the reading of the static strain testing system was calibrated by the pressure testing machine before the experiment. The steel strands were connected with cross-links of a certain stiffness at 1/10 *L*, 1/2 *L* and 9/10 *L* from the left end of the steel strand. The cross-link stiffnesses were also measured by the pressure testing machine before the experiment. The stiffness of the rigid cross-links was 10^7 N/m, as shown in Fig. 6(b), and the stiffness of the flexible cross-links was 10^4 N/m, as shown in Fig. 6(c).

Fig. 5. Panorama of the field experiments.

(a) (b) (c)

Fig. 6. Local layout of the experimental instruments: (a) pressure sensor; (b) rigid cross-link; (c) flexible cross-link.

After tensioning is completed, an acceleration sensor was placed on each steel strand to measure each strand's natural frequency. After conversion by a dynamic strain gauge connected to an acceleration sensor, the natural frequency was read from the spectrum displayed by the dynamic strain test system on a computer. Fig. 7 shows the system spectrum, with four cables and three cross-links, when the stiffness of the cross-links was 10^4 N/m. The first 10 natural frequencies read from the spectra were shown as f_{s3} in Table 2. The natural frequencies of each order in each steel strand were the same, which proves that the vibration of each cable in the cable network was consistent.

In Table 2, the maximum error between the first 10 natural frequencies, measured by the experimental method, and the first 10 natural frequencies, calculated by the analytical algorithm in this paper, is 4.82 % when the stiffness of the cross-link is $k_1 = 10^7$ N/m. The maximum error between the first 10 natural frequencies, measured by the experimental method, and the first 10 natural frequencies, calculated by the analytical algorithm in this paper, is −3.95 % when the stiffness of the

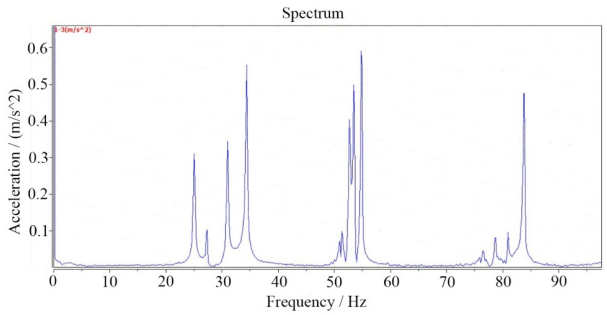

Fig. 7. Spectrum of the system with four cables and three cross-links (k = 10^4 N/m).

cross-link is $k_2 = 10^4$ N/m, which verifies the correctness of the theoretical derivation.

4. Effect of bending stiffness on the free vibration characteristics of a multilayer unequal stay-cable network

Taking five typical stay cables of a cable-stayed bridge as the analysis object, the stay cables' bending stiffness' influence on the cable network's free vibration characteristics was studied with different parameters. Because the cables selected are short, bending stiffness has a greater impact, whereas sag has a smaller impact. The error caused by the sag of each cable is less than 0.5 %, so the influence of sag is ignored [38]. To better summarize the rule, the geometric characteristics of each cable are consistent, as shown in Table 3, while the length, tensile force, and natural frequency of each cable without cross-ties are shown in Table 4 for the case that the cables are arranged symmetrically.

4.1 Effect of bending stiffness on the free vibration characteristics of stay-cable network

In the case of one cross-tie, the cross-tie was fixed at L/2 on the target cable, with its stiffness value set at 10^7 N/m, as shown in Fig. 8. To study how the frequency and the mode shape of the system changed with the cable's bending stiffness, the first four frequencies and modes of the cable network were examined without considering the cable's bending stiffness (EI = 0), considering part of the cable's bending stiffness (0.01EI, 0.1EI), and considering the entire cable's bending stiffness (EI), as shown in Fig. 9.

In the first four modes, as the cable's bending stiffness increased, the frequency of the corresponding order also increased. When the cable's bending stiffness was not considered, the first-order mode was the global vibration mode, the second-order mode was the local vibration mode of cable 1 and cable 2, the third-order mode was the single-cable vibration mode of cable 1, and the fourth-order mode was the single-cable vibration mode of cable 2. When considering part of or the entire cable's bending stiffness, since the frequency of

Table 3. Cable parameters of stay-cable network.

Cross-sectional area (m^2)	Inertia moment (m^4)	Elastic modulus (Pa)	Linear density (kg/m)
7.854×10^{-3}	4.909×10^{-6}	1.95×10^{11}	60

Table 4. Cable length, tensile force, and single cable frequency without cross-ties.

Cable number	Cable length (m)	Tensile force (kN)	Frequency (Hz)
Cable 1 (target cable)	100	3500	1.2205
Cable 2	96	3500	1.2719
Cable 3	92	3500	1.3279
Cable 4	88	3500	1.3890
Cable 5	84	3500	1.4560

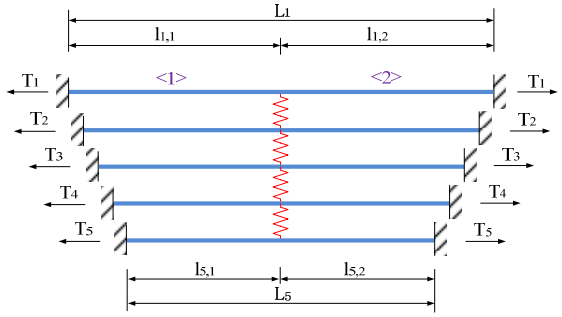

Fig. 8. Layout of the stay-cable network with five cables and single cross-tie.

the single-cable vibration mode of cable 1 increased more than that of the local vibration mode of cable 1 and cable 2, the second-order mode changed into the single-cable vibration mode of cable 1, the third-order mode changed into the local vibration mode of cable 1 and cable 2, and the first- and fourth-order mode did not change.

Fig. 10 shows the increased percentages (r_1) of the first 20 natural frequencies of the cable network when considering the cable's bending stiffness relative to those when the cable's bending stiffness is not considered.

When the cable's bending stiffness was 0.01EI, 0.1EI, and EI, the cable network's fundamental frequencies were 0.09 %, 0.36 %, and 1.17 % higher, respectively, than those when the cable's bending stiffness was not considered. Meanwhile, the first 20 natural frequencies of the network system were 0.19 %, 0.76 %, and 2.71 % higher, respectively, than those when the cable's bending stiffness was not considered. In addition, when considering the entire cable's bending stiffness, the target cable's fundamental frequency increased by 8.77 % compared with the fundamental frequency when no cross-ties were applied. For the multilayer unequal stay-cable network, the stiffness of the target cable clearly increased after applying the cross-tie.

In the first 20 modes, the first- and eleventh-order modes were the global vibration modes, while the remaining modes

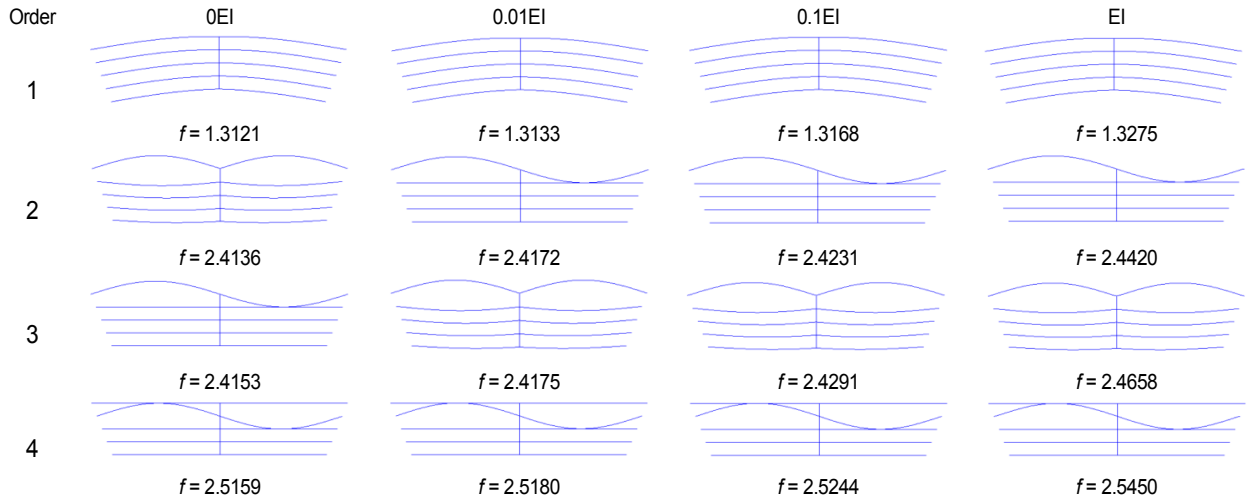

Fig. 9. Changes in the first four frequencies and the mode shapes of the system with the cable's bending stiffness.

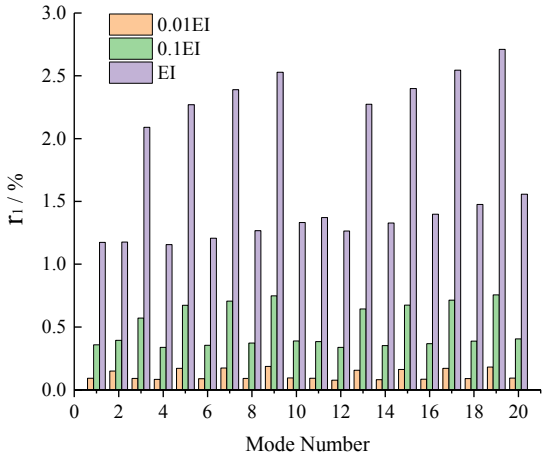

Fig. 10. Increase in the percentage of the first 20 natural frequencies of the cable network when considering the cable's bending stiffness.

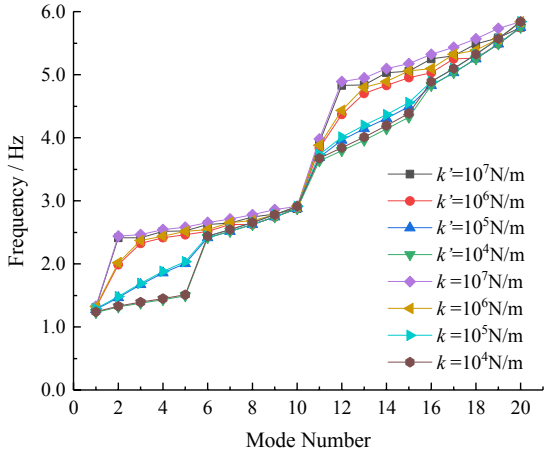

Fig. 11. Curves of the first 20 natural frequencies in the stay-cable network, indicating the changes with the stiffness of the cross-tie.

were local vibration modes. When the cable's bending stiffness was not considered, the 2nd, 5th, 7th, 9th, 13th, 15th, 17th, and 19th modes were multiple-cable local vibration modes, while the 3rd, 4th, 6th, 8th, 10th, 12th, 14th, 16th, 18th, and 20th modes were single-cable vibration modes only. After considering part of or the entire cable's bending stiffness, the vibration modes of the other orders underwent no change, with the exception of the 2nd mode, which changed to a single-cable vibration mode, and the 3rd mode, which changed to a multiple-cable local vibration mode.

4.2 Effect of bending stiffness on the free vibration characteristics of a cable network with different cross-tie stiffnesses

When there is one cross-tie, it is fixed at L/2 on the target cable. By changing the cross-tie stiffness, the cross-tie stiffness values are 10^7, 10^6, 10^5, and 10^4 N/m. The first 20 frequencies f' in the cable network, while not considering the cable's bending stiffness and the first 20 frequencies f in the cable network, while considering the entire cable's bending stiffness, are as shown in Fig. 11.

When the cross-tie stiffness was 10^6 N/m, and the cable's bending stiffness was not considered, the cable network's fundamental frequency was 1.3078 Hz, while when the entire cable's bending stiffness was considered, the frequency was 1.3230 Hz, which represented a 1.16 % increase. The first 20 natural frequencies were up to 2.40 % higher when considering the entire cable's bending stiffness than when not considering this factor. Meanwhile, the local vibration frequencies of the multiple cables were smaller for a cross-tie stiffness of 10^7 N/m, while the single-cable's vibration frequency did not change with the changes in the cross-tie stiffness. Therefore, in the first 20 modes, the first- and eleventh-order mode remained the global vibration modes. When the cable's bending stiffness was not considered, the multiple cables'

local vibration modes moved forward to the 2nd, 3rd, 5th, 7th, 12nd, 13th, 15th, and 18th order modes, relative to a cross-tie stiffness of 10^7 N/m, with the remaining modes being the single-cable vibration modes. When considering the entire cable's bending stiffness, the vibration modes of the remaining orders did not change, with the exception of a switch between the 7th and 8th modes.

The same rule also applied when the cross-tie stiffness was 10^5 and 10^4 N/m. At these levels of stiffness, the cable network's fundamental frequencies, without considering the cable's bending stiffness, were 1.2760 and 1.2286 Hz, respectively. Meanwhile, the cable network's fundamental frequencies when considering the entire cable's bending stiffness were 1.2899 and 1.2417 Hz, indicating a 1.09 % and 1.07 % increase with respect to the values when the cable's bending stiffness was not considered. The first 20 natural frequencies when considering the entire cable's bending stiffness were both up to 1.56 % higher than those when the cable's bending stiffness was not considered. Moreover, the global and local vibration frequencies of the multiple cables further decreased. When the cable's bending stiffness was not considered, the multiple cables' local vibration modes moved forward to the 2nd, 3rd, 4th, 5th, 12nd, 13th, 14th, and 15th order modes, with the remaining modes being single-cable vibration modes. When considering the entire cable's bending stiffness, the vibration modes of all the orders did not change.

Thus, for a system with five-cables and a single cross-tie, under the same cross-tie stiffness, the frequency of the network system will increase as the cable's bending stiffness increases, and the order of modes will undergo a slight change but the shapes will not change. As the cross-tie stiffness decreased, the increasing percentage of the frequencies when considering the bending stiffness also decreased compared with those when the bending stiffness was not considered. In addition, with the same bending stiffness, the global vibration frequencies and the local vibration frequencies of multiple cables will decrease as the cross-tie stiffness decreases, but the individual vibration frequencies of single cables will not change as the cross-tie stiffness changes, so the stiffness of the cable network decreases as the cross-tie stiffness decreases. Furthermore, the multiple cables' local vibration modes will move forward as the cross-tie stiffness decreases. When the cross-tie stiffness was 10^4 N/m, the fundamental frequency when considering the entire cable's bending stiffness was 6.46 % less than the frequency when the cross-tie stiffness was 10^7 N/m.

4.3 Effect of bending stiffness on the free vibration characteristics of a cable network with different cross-tie positions

For a single cross-tie, the cross-tie stiffness is 10^7 N/m. By changing the cross-tie positions, the positions of the cross-ties

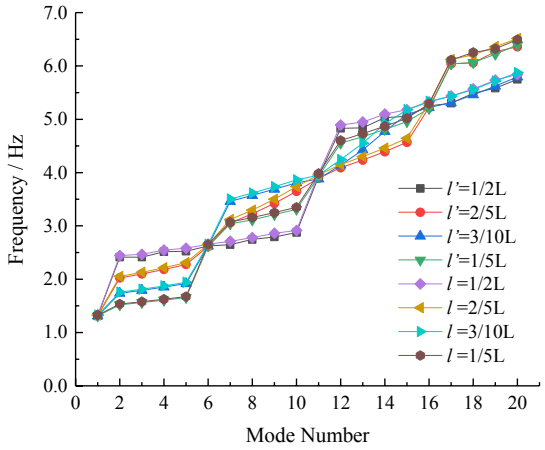

Fig. 12. Curve of the first 20 natural frequencies in the stay cable network, indicating the changes with the position of the cross-tie.

are at 1/2 *L*, 2/5 *L*, 3/10 *L,* and 1/5 *L* from the left end of the target cable. The first 20 frequencies *f'* in the cable network, while not considering the cable's bending stiffness and the first 20 frequencies *f* in the cable network, while considering the entire cable's bending stiffness, are as shown in Fig. 12.

When the cross-tie was located at 2/5 *L*, 3/10 *L,* and 1/5 *L* on the target cable, the cable network's fundamental frequencies, when not considering the cable's bending stiffness, were 1.3121, 1.3118, and 1.3108 Hz, respectively. Meanwhile, the cable network's fundamental frequencies when considering the entire cable's bending stiffness were 1.3275, 1.3273, and 1.3265 Hz, respectively, representing a 1.17 %, 1.18 %, and 1.20 % increase compared with the values when the cable's bending stiffness was not considered. The first 20 natural frequencies were up to 2.46 %, 3.07 %, and 3.09 % higher when considering the entire cable's bending stiffness than when this factor was not considered. In the first 20 modes, the 1st, 6th, 11th, and 16th order modes were the global vibration modes, while the remaining modes were the local vibration modes; however, there were no single-cable vibration modes. When considering the entire cable's bending stiffness, the vibration modes of all the orders did not change.

Thus, for the system with five cables and a single cross-tie, owing to the special condition of the cross-tie being in the middle of the cable, there were local vibration modes for the multiple cables and individual vibration modes for the single cables between the global vibration modes. However, when the cross-tie was at a position other than the center of the cable, individual vibration modes of the single cables did not appear. In the same cross-tie position, the frequency of the network system will increase as the cable's bending stiffness increases. With the exception of when the cross-tie is located at *L*/2 on the target cable, the vibration mode will not change after considering the cable's bending stiffness, while, as the position of the cross-tie approaches the anchor point, the increasing percentage of the frequencies when considering the bending stiffness will increase compared with those when not considering the

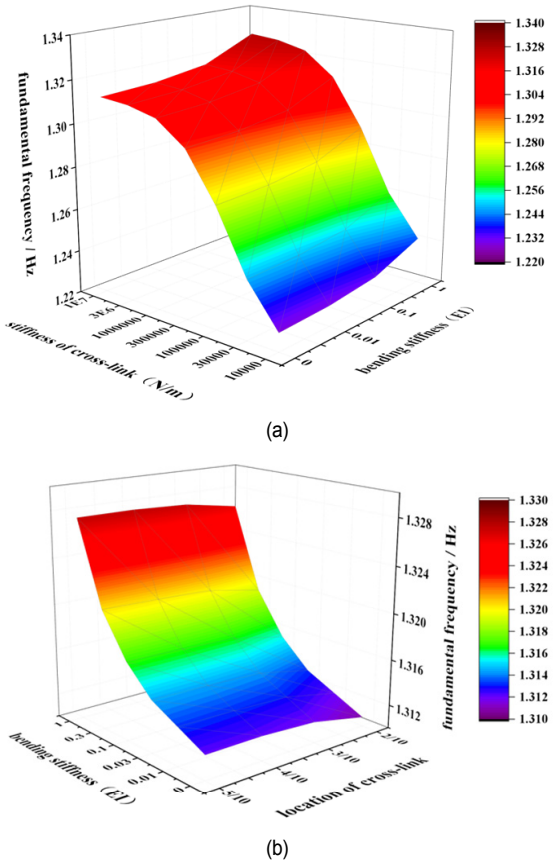

Fig. 13. Cable network's fundamental frequency diagram: (a) cable network's fundamental frequency diagram under the interaction between cable's bending stiffness and cross-tie stiffness (l = L/2); (b) cable network's fundamental frequency diagram under the interaction between cable's bending stiffness and cross-ties position (k = 10^7 N/m).

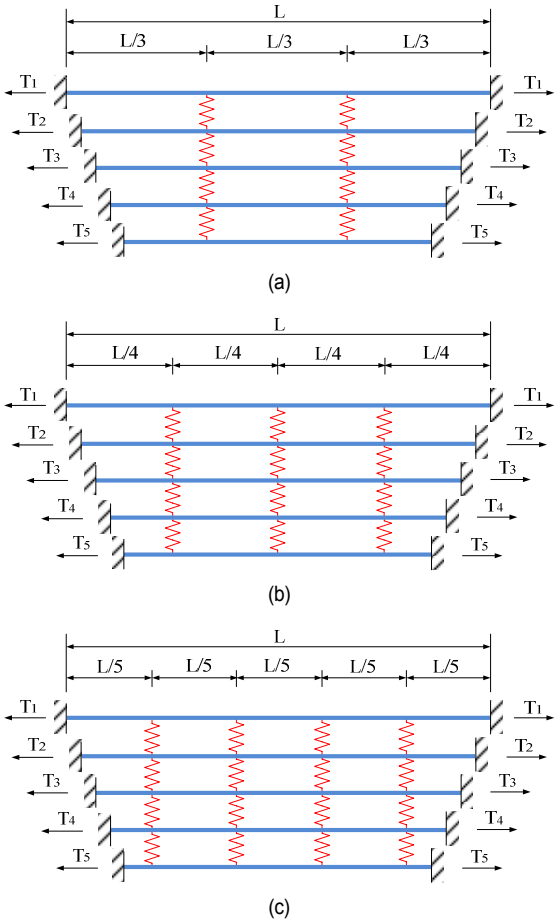

Fig. 14. Structure layout of five-cable and multi-cross-ties stay cable network: (a) two cross-ties system; (b) three cross-ties system; (c) four cross-ties system.

bending stiffness, such that the effect of bending stiffness on the frequency of the cable network system increases. In addition, with the same bending stiffness, the fundamental frequency slightly decreases as the position of the cross-tie approaches the anchor point, but this change can generally be ignored. When the cross-tie was located at 1/5 *L* on the target cable, the fundamental frequency when considering the entire cable's bending stiffness was 0.08 % lower than the frequency when the cross-tie was located at *L*/2 on the target cable; this effect was not clear. The frequencies of the global vibration modes were less affected by the relative position and were almost the same, while the frequencies of the local vibration modes were affected by the cross-tie position and exhibited a level of variation, as shown in Fig. 12.

When the cross-tie is located at L/2 on the target cable, the surface plot of the cable network's fundamental frequencies, while considering the interaction between the cable's bending stiffness and the cross-tie stiffness, is shown in Fig. 13(a). When the cross-tie stiffness is 10^7 N/m, the surface plot of the cable network's fundamental frequencies, while considering the interaction between the cable's bending stiffness and the position of the cross-tie, is shown in Fig. 13(b). The cable network's fundamental frequency decreases with decreases in the cable's bending stiffness, and also decreases with decreases in the cross-tie stiffness; at the same time, the fundamental frequency decreases as the cross-tie's position becomes closer to the anchor point. However, the influence of the cross-tie stiffness is greater, followed by the cable's bending stiffness, and the cross-tie position has the least impact. Therefore, the cross-tie stiffness should be as great as possible, and the effect of the cross-tie position on the fundamental frequency is almost negligible.

4.4 Effect of bending stiffness on the free vibration characteristics of a cable network with different number of cross-ties

With the cross-ties stiffness was maintained at 10^7 N/m, the number of cross-ties was changed to either 2, 3, or 4. The position of each cross-tie was evenly distributed along the target cable, with the distance between adjacent cross-ties being L/(n+1) on the target cable, as shown in Fig. 14.

The first 20 frequencies *f'* in the cable network when not considering the cable's bending stiffness and the first 20 fre-

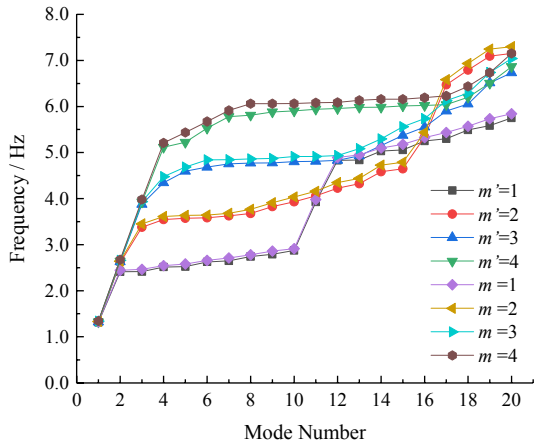

Fig. 15. The curve of the first 20 natural frequencies of the stay-cable network changing with the number of the cross-ties.

quencies *f* in the cable network when considering the entire cable's bending stiffness, were as shown in Fig. 15.

When there were two cross-ties, the first- and second-order mode shapes were the global vibration modes, whereas the remaining modes of the first 20 orders were multiple-cable local vibration modes. When considering the entire cable's bending stiffness, the modes were the same as those when not considering the cable's bending stiffness. The cable network's fundamental frequency was 1.3174 Hz, and the minimum frequency of the local vibrations was 3.3789 Hz when not considering the cable's bending stiffness, while when considering the entire cable's bending stiffness, the fundamental frequency was 1.3329 Hz, representing a 1.18 % increase. The minimum frequency of the local vibrations when considering the entire cable's bending stiffness was 3.4508 Hz, a 2.13 % increase in the frequency when not considering the cable's bending stiffness. The first 20 natural frequencies when considering the entire cable's bending stiffness were up to 3.15 % higher than those when not considering the cable's bending stiffness.

When there were three cross-ties, the first- to third-order mode shapes were the global vibration modes, while the remaining modes of the first 20 orders were multiple-cable local vibration modes. When considering the entire cable's bending stiffness, the mode shapes will not change but the order of the 6th-12th modes will change. The cable network's fundamental frequency was 1.3212 Hz and the minimum frequency of the local vibrations was 4.3439 Hz when not considering the cable's bending stiffness, whereas when considering the entire cable's bending stiffness, the fundamental frequency was 1.3371 Hz, representing a 1.20 % increase. The minimum frequency of the local vibrations when considering the entire cable's bending stiffness was 4.4772 Hz, a 3.07 % increase over that when not considering the cable's bending stiffness. When considering the entire cable's bending stiffness, the first 20 natural frequencies were up to 4.58 % higher than those when the cable's bending stiffness was not considered.

For the case of four cross-ties, the first-fourth order mode shapes were the global vibration modes, while the remaining modes of the first 20 orders were multiple-cable local vibration modes. After considering the entire cable's bending stiffness, the mode shapes will not change but the order of the 7th-17th modes will. Without considering the cable's bending stiffness, the cable network's fundamental frequency was 1.3250 Hz and the minimum frequency of the local vibrations was 5.2226 Hz, whereas when considering the entire cable's bending stiffness, the cable network's fundamental frequency was 1.3413 Hz, representing a 1.23 % increase. The minimum frequency of the local vibrations when considering the entire cable's bending stiffness was 5.4348 Hz, a 4.06 % increase over the frequency when the cable's bending stiffness was not considered. The first 20 natural frequencies when considering the entire cable's bending stiffness were up to 4.26 % higher than those when the cable's bending stiffness was not considered.

Thus, for a system with five-cables, in the case where the number of cross-ties is the same, the frequency of the network system will increase as the cable's bending stiffness increases and the order of some of the modes will undergo a slight change, but the shapes will not change. As the number of cross-ties increases, the increasing percentage of the frequencies when considering the bending stiffness will also increase compared with those when not considering the bending stiffness, such that the effect of bending stiffness on the frequencies of the cable network system increases. In addition, in the case where the cable's bending stiffness is the same, the greater the number of cross-ties, the larger the cable network's fundamental frequency. When the number of cross-ties was 2, 3, or 4, the cable network's fundamental frequencies when considering the entire cable's bending stiffness were 0.41 %, 0.72 % and 1.04 % higher, respectively, than when the number of cross-ties was 1. When the number of cross-ties is *n*, the first *n* order mode shapes are the global vibration modes. As the number of cross-ties increases, the later that the local vibration mode shape appears, the larger the minimum frequency of the local vibration is.

When the stiffness of the cross-tie is 10^7 N/m, the fundamental frequency surface diagram of the cable network, while considering the interactions between the cable's bending stiffness and the number of cross-ties, is shown in Fig. 16. The cable network's fundamental frequency decreases with a decrease of the cable's bending stiffness, and also increases with an increase in the number of cross-ties. Moreover, basically, the increase in the fundamental frequency is linear with increases in the number of cross-ties.

4.5 Effect of bending stiffness on the free vibration characteristics of a cable network with different number of cables

To understand the generality of the number of cables, the cross-tie position is located at 3/10 *L* on the target cable. When

Table 5. Comparison of the first five frequencies and modes of the system under different cable numbers (Hz).

Order	Five cables			Four cables			Three cables			Two cables		
	Without considering bending stiffness	Considering bending stiffness	Mode shape	Without considering bending stiffness	Considering bending stiffness	Mode shape	Without considering bending stiffness	Considering bending stiffness	Mode shape	Without considering bending stiffness	Considering bending stiffness	Mode shape
1	1.3118	1.3273	GM	1.2844	1.2991	GM	1.2579	1.2719	GM	1.2322	1.2457	GM
2	1.7359	1.7560	LM	1.7379	1.7581	LM	1.7409	1.7612	LM	1.7461	1.7665	LM
3	1.7914	1.8128	LM	1.7950	1.8165	LM	1.8009	1.8226	LM	2.4645	2.4924	GM
4	1.8513	1.8742	LM	1.8577	1.8808	LM	2.5154	2.5448	GM	3.4840	3.5267	LM
5	1.9175	1.9421	LM	2.5679	2.5989	GM	3.4728	3.5154	LM	3.6950	3.7421	GM

GM is global vibration mode; LM is local vibration mode

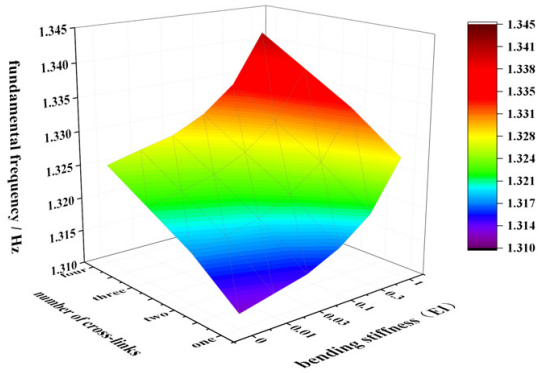

Fig. 16. Cable network's fundamental frequency diagram under the interaction of the cable's bending stiffness and the number of cross-ties.

the stiffness of the cross-tie is kept at 10^7 N/m, the number of cables is changed to 4, 3, and 2 and the order of reduction is from short to long. The layout of each system is shown in Fig. 17. The first five frequencies of the cable network without considering the cable's bending stiffness and considering the entire cable's bending stiffness are obtained, as given in Table 5. In addition, the first five mode shapes of the cable network, with different numbers of cables, are determined, as shown in Fig. 18.

When the number of cables was 5, 4, 3, and 2, the cable network's fundamental frequencies without considering the cable's bending stiffness were 1.3118, 1.2844, 1.2579, and 1.2322 Hz, respectively. Moreover, the cable network's fundamental frequencies when considering the entire cable's bending stiffness were 1.3273, 1.2991, 1.2719, and 1.2457 Hz, respectively, representing a 1.18 %, 1.14 %, 1.11 %, and 1.10 % increase over the frequencies when not considering the cable's bending stiffness. In the first five modes, when the number of cables was 5, the first-order mode was the global vibration mode and the second-fifth-order modes were the local vibration modes. When the number of cables was 4, the first- and fifth-order modes were the global vibration modes and the second-fourth-order modes were the local vibration modes. When the number of cables was 3, the first- and fourth-order

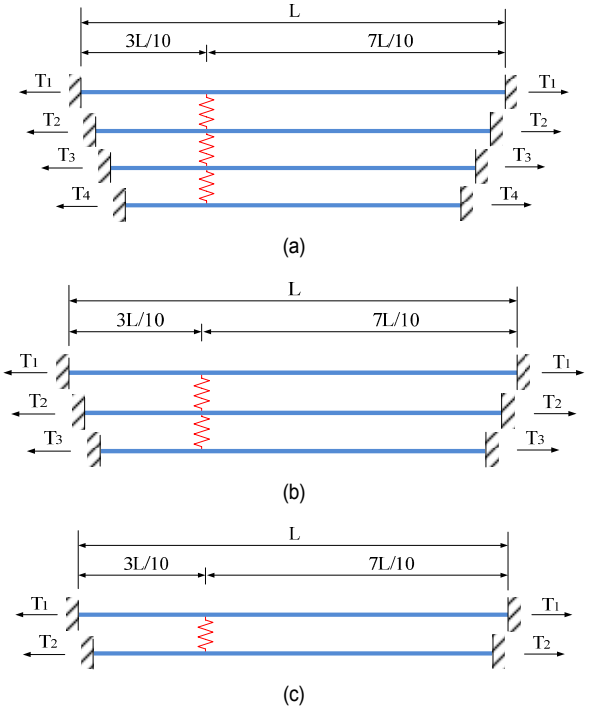

Fig. 17. Structure layout of multi-cables and single cross-tie stay cable network: (a) four cables system; (b) three cables system; (c) two cables system.

modes were the global vibration modes and the second-, third-, and fifth-order modes were the local vibration modes. When the number of cables was 2, the first-, third-, and fifth-order modes were the global vibration modes and the second- and fourth-order modes were the local vibration modes. When considering the entire cable's bending stiffness, the vibration modes of all the orders did not change compared with those when the cable's bending stiffness was not considered.

Thus, for a system with five-cables, in the case where the number of cables is the same, the frequency of the network system will increase as the cable's bending stiffness increases, while the vibration mode will not change. As the number of cables decreases, the increasing percentage of the frequencies

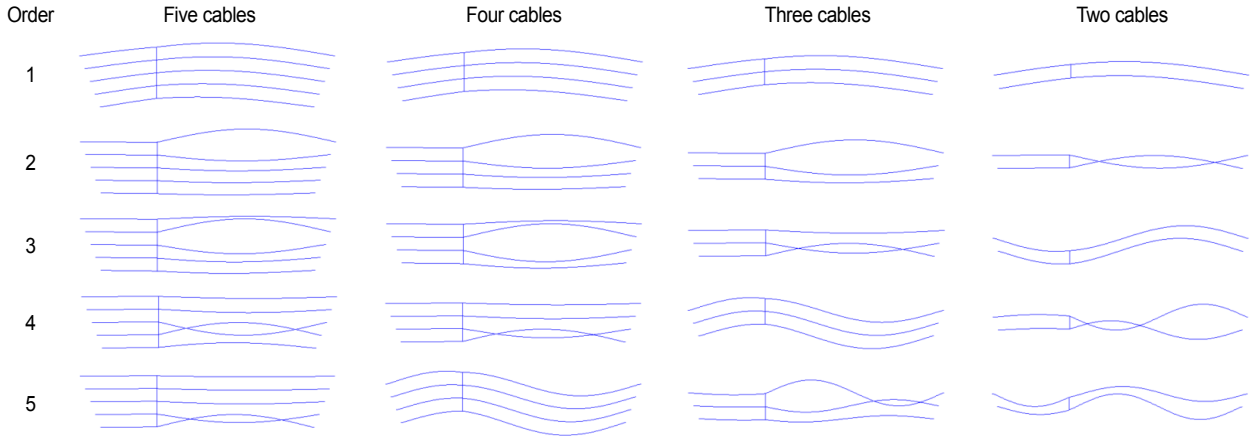

Fig. 18. First five mode shapes of the system with multi-cable and single cross-tie.

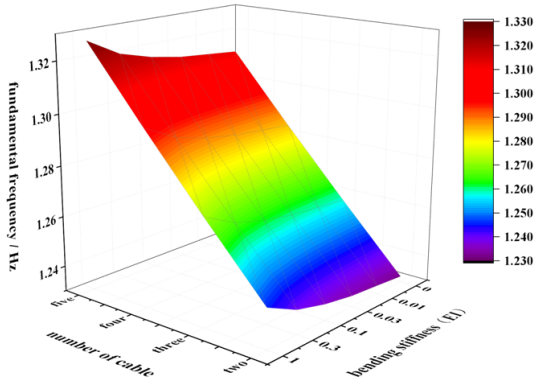

Fig. 19. Cable network's fundamental frequency diagram under the interaction between the cable's bending stiffness and the number of cables.

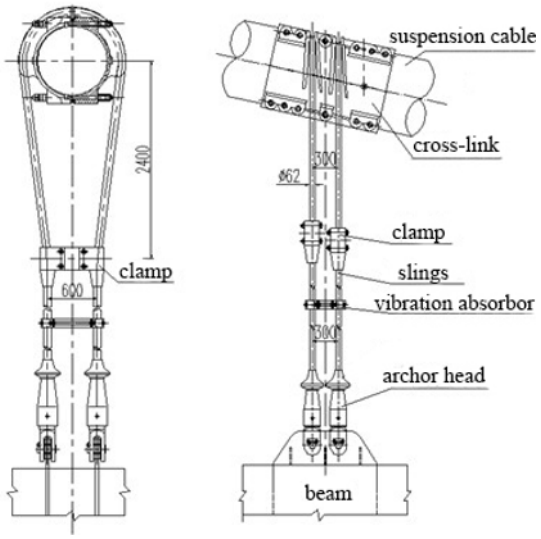

Fig. 20. Diagram of the sling structure.

when considering the bending stiffness will also decrease compared with that when not considering the bending stiffness, such that the effect of bending stiffness on the frequency of cable network system decreases. In addition, in the case where the cable's bending stiffness is the same, since the cable lengths increase successively from cable 5 to cable 1, the cables' free vibration frequncies will decrease successively, from cable 5 to cable 1, when the cables are not connected by cross-ties. Therefore, the lower the number of the cables, the smaller the cable network's fundamental frequency. A certain number of local vibration modes will appear between the global vibration modes. When the number of cables is 5, 4, 3, or 2, there will be 4, 3, 2, or 1 local vibration modes, respectively, between the global vibration modes. Therefore, there will be (n–1) local vibration modes between the global vibration modes in the n cable system.

The fundamental frequency surface diagram of the cable network, while considering the interactions between the cable bending stiffness and the number of cables, is shown in Fig. 19. The cable network's fundamental frequency decreases with reduction in the cable bending stiffness, and also decreases with decreases in the number of cables. Moreover, basically, the decrease in the fundamental frequency is linear with decreasing numbers of cables.

5. Effect of bending stiffness on the free vibration characteristics of a double-layer equal-sling network

To study the influence of the bending stiffness of the slings on the sling network's in-plane free vibration characteristics with different parameter systems, the slings at the C21L, C12L, and C03L suspension points of the Aizhai Large Suspension Bridge were used as the analysis object. The sling structure is shown in Fig. 20. There are four slings at each suspension point, and the slings straddle the suspension cable connected by the cross-links. Two slings in the transverse direction of the bridge are connected by a clamp at the top, and all of the slings are anchored to the beam by the anchor head at the bottom. The vibration absorber is set between the slings. The sling

length between the clamp and the anchor head is taken as the operating sling length, the operating sling length L_A of C21L is 17.700 m, the operating sling length L_B of C12L is 42.048 m, the operating sling length L_C of C03L is 79.176 m. The two slings in the longitudinal direction of the bridge are considered equivalent to the same sling. Therefore, there are double layers and equal-length slings in the transverse direction of the bridge connected by the vibration absorber. We analyze its in-plane free vibration characteristics in the transverse direction of the bridge. The analysis model is shown in Fig. 21.

The sling forces T1 = T2 = 1000 kN, and each sling's geometric characteristics, are shown in Table 6. The sling frequency value of C21L is 5.189 Hz, the sling frequency value of C12L is 2.126 Hz and the sling frequency value of C03L is 1.120 Hz when the vibration absorber is not installed.

Table 6. Parameters of slings.

Cross-sectional area (m^2)	Inertia moment (m^4)	Elastic modulus (Pa)	Linear density (kg/m)
3.895×10^{-3}	1.207×10^{-6}	1.15×10^{11}	32.46

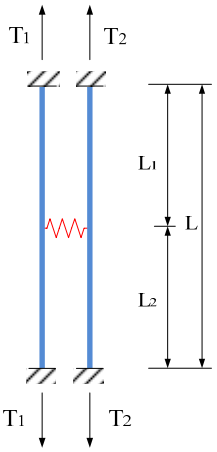

Fig. 21. Layout of the sling network.

5.1 Effect of bending stiffness on the free vibration characteristics of a sling network

When the vibration absorber is located at L/2 on the sling, and the vibration absorber stiffness is 10^7 N/m, to study how the frequency and mode shape of the system change with the sling's bending stiffness, the first four frequencies and modes of the C12L (L_B = 42.048 m) network without considering the sling's bending stiffness (EI = 0), considering part of sling's bending stiffness (0.01EI, 0.1EI) and considering the entire sling's bending stiffness (EI), are as shown in Fig. 22.

In the first four modes, as the sling's bending stiffness increased, the frequency of the corresponding order increased. When the sling's bending stiffness was not considered and when considering a 0.01 times the sling's bending stiffness, the first-order mode was the in-phase global vibration mode, the second-order mode was the out-of-phase global vibration mode, and the third- and fourth-order modes were the single vibration mode of sling 1 and sling 2, respectively. When considering a 0.1 times the sling's bending stiffness and the entire sling's bending stiffness, given that the frequency of the single vibration mode of sling 1 and sling 2 increased more than that of the out-of-phase global vibration mode, the second- and third-order modes changed into the single vibration mode of sling 1 and sling 2, respectively, while the fourth-order mode changed into the out-of-phase global vibration mode.

The increased percentages (r_2) of the first 20 natural frequencies of the C12L network considering the sling's bending stiffness compared with that without considering the sling's bending stiffness are shown in Fig. 23.

When the sling's bending stiffness was 0.01EI, 0.1EI, and EI, the sling network's fundamental frequencies were 0.19 %, 0.57 %, and 1.87 % higher, respectively, than those without considering the sling's bending stiffness. The first 20 natural

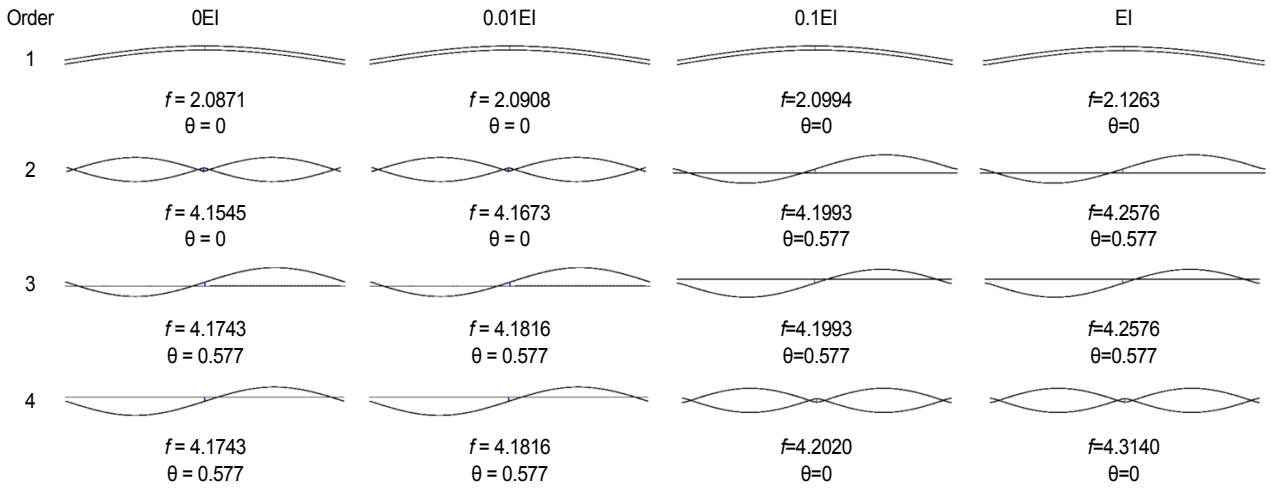

Fig. 22. The first four frequencies and mode shapes of the system changing with the sling's bending stiffness.

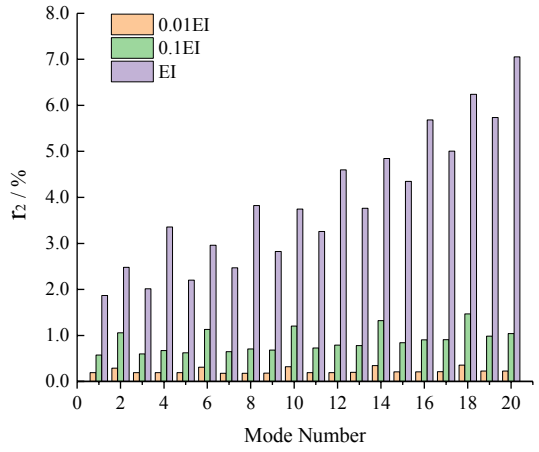

Fig. 23. Increased percentage of the first 20 natural frequencies of the C12L network considering the sling's bending stiffness.

frequencies of the network system were up to 0.36 %, 1.47 %, and 7.05 % higher, respectively, than those without considering the sling's bending stiffness. In addition, when considering the entire sling's bending stiffness, the sling network's fundamental frequency was still 2.126 Hz, which is the same frequency present without setting the vibration absorber. Therefore, the application of the vibration absorber to the double-layer equal-length sling does not change the sling network's fundamental frequency.

For the special case that the vibration absorber is located in the middle of the sling, the distribution curve of the sling network frequencies presents a "stair-step" pattern that every fourth order is one period of change. When the sling's bending stiffness is not considered and considering 0.01 times the sling's bending stiffness, the 1st order in a period is an in-phase global vibration mode, and the 2nd order is an out-of-phase global vibration mode, and the 3rd and 4nd orders are individual vibration modes of a single sling. The frequencies of the individual vibrations of a single sling in each period are the same, and the frequencies of the out-of-phase global vibrations are smaller than the individual vibrations of a single sling. When considering 0.1 times the sling's bending stiffness and the entire sling's bending stiffness, the order of the in-phase global vibrations does not change and is still the 1st order in a period, but the frequencies of the individual vibrations of a single sling become smaller than those of out-of-phase global vibrations and move forward to the 2nd and 3rd orders, so the 4th orders is an out-of-phase global vibration mode.

To assess the distinction between the global and local modes, Zhou [27] provided a more appropriate means to distinguish the global mode and local mode using potential energy of each cable segment and assessed the degree of mode localization using the energy distribution of each cable segment.

The mode energy distribution vector is defined as

$$E = [E_{11} \quad E_{12} \quad E_{21} \quad E_{22}] \tag{39}$$

where E_{ij} is the nondimensional potential vibration mode energy of the cable i and subsystem j. These can be derived by calculating the potential vibration mode energy from the known mode shape.

$$U_{ij} = \frac{T_i}{2}\int_0^{l_{ij}} \left(\frac{\partial \varphi_i^{<j>}}{\partial x_{ij}} \right)^2 dx_{ij} \tag{40}$$

$$E_{ij} = \frac{U_{ij}}{\sum_{i=1}^{n}\sum_{j=1}^{m} U_{ij}} . \tag{41}$$

The mode energy distribution vector can clearly indicate the vibration mode energy distribution of each segment, but it cannot offer a simple and direct way of identifying the global and local modes. Therefore, we must use the nondimensional index θ to measure the degree of mode localization:

$$\theta = \sqrt{\frac{N}{N-1}} \sqrt{\sum_{i=1}^{n}\sum_{j=1}^{m} \left(E_{ij} - \frac{1}{N} \right)^2} \tag{42}$$

where N is the total number of cable segments. The vibration mode will be more "local" as θ increases. When the vibration absorber is located at L/2 on the sling and when the mode is the in-phase or the out-of-phase global vibration mode, θ = 0, and when the mode is the individual vibrations mode of a single sling, θ = 0.577. The values of θ are also listed in Fig. 22, a clear identification of the local mode when θ is greater than 0.5.

5.2 Effect of bending stiffness on the free vibration characteristics of a sling network with different sling lengths

When the vibration absorber was located at L/2 on the sling and the vibration absorber stiffness was 10^7 N/m, the frequencies of the C21L (17.700 m), C12L (42.048 m), and C03L (79.176 m) sling networks without considering and considering the bending stiffness can be denoted as f'_A, f'_B, f'_C, f_A, f_B, and f_C. The first 20 frequencies of the sling network are shown in Fig. 24, and the increased percentages (r_3) of the natural frequency when considering the entire slings' bending stiffness are shown in Fig. 25.

As Figs. 24 and 25 show, the network's fundamental frequency for the C21L sling network without considering the sling's bending stiffness was 4.958 Hz, while when considering the entire sling's bending stiffness, the frequency was 5.189 Hz, representing a 4.66 % increase. When considering the entire sling's bending stiffness, the first 20 natural frequencies were up to 27.01 % higher than those when the sling's bending stiffness was not considered. For the C03L sling network, the network's fundamental frequency without considering the sling's bending stiffness was 1.108 Hz, while when considering the entire sling's bending stiffness, the frequency was 1.120 Hz, representing a 1.08 % increase. When considering the entire

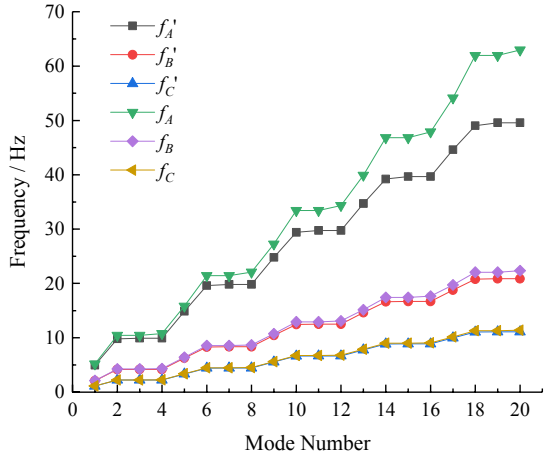

Fig. 24. Curve of the first 20 natural frequencies of the sling network.

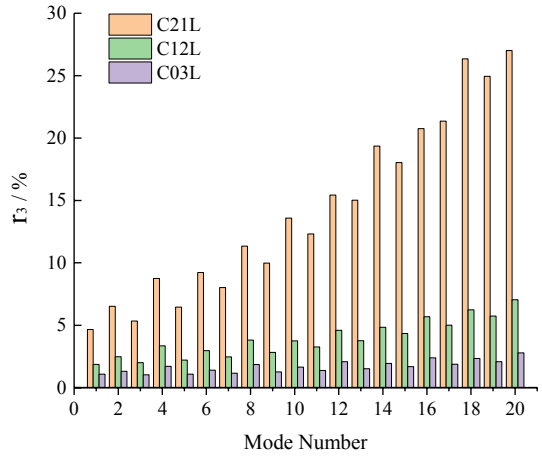

Fig. 25. Increase in percentage of the first 20 natural frequencies of the sling network when considering the entire sling's bending stiffness.

sling's bending stiffness, the first 20 natural frequencies were up to 2.79 % higher than those when the sling's bending stiffness was not considered.

For the C21L and C03L sling networks, owing to the special case of the vibration absorber being located in the middle of the sling, when the sling's bending stiffness was not considered, the distribution curve of the sling network frequencies exhibited a "stair-step" pattern wherein every fourth order was one period of change from the C12L sling network. The first order in a given period was an in-phase global vibration mode, the second order was an out-of-phase global vibration mode, and the third and fourth orders were individual vibration modes of a single sling. When considering the entire sling's bending stiffness, the distribution curve of the sling network frequencies exhibited a "stair-step" pattern wherein every fourth order was one period of change from the C12L sling network. The order of the in-phase global vibrations did not change and remained the first order in a given period, whereas the frequencies of the individual vibrations of a single sling became smaller than those of the out-of-phase global vibrations and moved forward to the second and third orders, resulting in the fourth order being an out-of-phase global vibration mode.

Thus, for a system with two slings and a single vibration absorber, in the case where the sling length is the same, the frequency of the network system will increase as the cable's bending stiffness increases. When the sling's bending stiffness is not considered, the frequency of each order of the in-phase global vibrations and the individual vibrations of a single sling will increase by integral multiples. After the sling's bending stiffness is considered, the frequency of each order of the in-phase global vibrations and individual vibrations of a single sling do not increase by integral multiples, and exchange the order of out-of-phase global vibrations and individual vibrations of a single sling. Besides, as the sling length decreases, the increasing percentage of the frequencies, while considering the bending stiffness, increase compared to those without considering the bending stiffness. As the length of the sling becomes longer, the frequencies of each order of the in-phase global vibrations and individual vibrations of a single sling approach to increase by an integral multiple.

5.3 Effect of bending stiffness on the free vibration characteristics of a sling network with different stiffnesses of the vibration absorber

When the vibration absorber is located at L/2 on the sling, the vibration absorber stiffness is infinite, 10^7 N/m, 10^6 N/m, 10^5 N/m, and 10^4 N/m by changing the stiffness of the vibration absorber. The first 20 frequencies *f'* in the C12L (42.048 m) network, while not considering the sling's bending stiffness and the first 20 frequencies *f* in the C12L (42.048 m) network, while considering the entire sling's bending stiffness, are as shown in Fig. 26.

When the vibration absorber stiffness was infinite, the network's fundamental frequency without considering the sling's bending stiffness was 2.087 Hz, while when considering the entire sling's bending stiffness, the frequency was 2.126 Hz, representing a 1.87 % increase. The first 20 natural frequencies when considering the entire sling's bending stiffness were up to 7.68 % higher than those when the sling's bending stiffness was not considered. When the sling's bending stiffness was not considered, the distribution curve of the sling network frequencies exhibited a "stair-step" pattern wherein every fourth order was one period of change from the network with a vibration absorber stiffness of 10^7 N/m. The first order in a given period was an in-phase global vibration mode, the second order was an out-of-phase global vibration mode, and the third and fourth orders were individual vibration modes of a single sling. However, it is interesting to note that the frequencies of the out-of-phase global vibrations became equal to those of the individual vibrations of the single slings and did not exceed them. Therefore, when the sling's bending stiffness is not considered, changing the stiffness of the vibration absorber does not change the order of the mode shapes. When considering

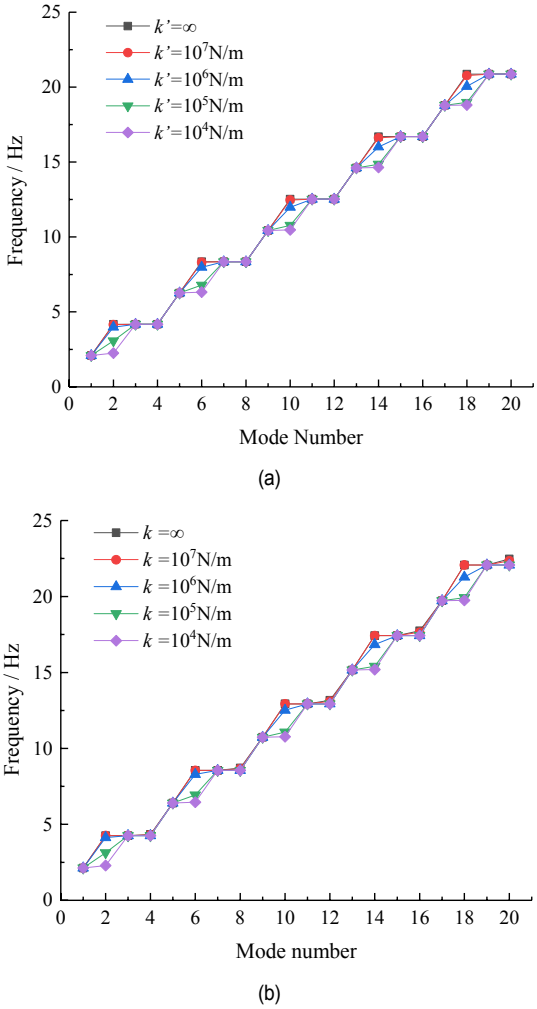

Fig. 26. The curve of the first 20 natural frequencies of the sling network changing with the vibration absorber stiffness: (a) the curve of the first 20 natural frequencies without considering the sling's bending stiffness; (b) the curve of the first 20 natural frequencies considering the entire sling's bending stiffness.

the entire sling's bending stiffness, the distribution curve of the sling network frequencies exhibited a "stair-step" pattern wherein every fourth order was one period of change. The order of the in-phase global vibrations did not change and remained the first order in a given period, whereas the frequencies of the individual vibrations of a single sling became smaller than those of the out-of-phase global vibrations and moved forward to the second and third orders, resulting in the fourth order being an out-of-phase global vibration mode.

When the vibration absorber stiffness was 10^6, 10^5, and 10^4 N/m, the first 20 natural frequencies when considering the entire sling's bending stiffness were up to 6.15 %, 5.73 %, and 5.73 % higher, respectively, than those when the sling's bending stiffness was not considered. When the vibration absorber stiffness was not greater than 10^6 N/m, the frequencies of the individual vibrations of a single sling did not become smaller than those of the out-of-phase global vibrations, when considering the entire sling's bending stiffness. Therefore, after considering the entire cable's bending stiffness, the vibration modes of all orders did not change. The distribution curve of the sling network frequencies exhibited a "stair-step" pattern wherein every fourth order was one period of change. The first order in a given period was an in-phase global vibration mode, the second order was an out-of-phase global vibration mode, and the third and fourth orders were individual vibration modes of a single sling.

Thus, for a system with two slings and a single vibration absorber, in the case where the vibration absorber stiffness is the same, the frequency of the network system will increase as the cable's bending stiffness increases. When the vibration absorber stiffness is more than 10^6 N/m, a "phenomenon of jump order" will appear after considering the entire sling's bending stiffness, and the order of the individual vibration modes of a single sling will move forward from the third and fourth order to the second and third order of each period. When the vibration absorber stiffness is not more than 10^6 N/m, the vibration modes of all orders when considering the entire sling's bending stiffness will be the same as those without considering the sling's bending stiffness. As the vibration absorber stiffness decreases, the increasing percentage of the frequencies when considering the bending stiffness will also decrease compared with those without considering the bending stiffness, such that the effect of the bending stiffness on the frequency of the cable network system decreases. In addition, in the case where the sling's bending stiffness is the same, the frequency of the in-phase global vibrations and the individual vibrations of a single sling remain unchanged, whereas the frequency of the out-of-phase global vibrations decreases with the decrease in the vibration absorber stiffness. Therefore, as the vibration absorber stiffness decreases, the stiffness of the sling network system also decreases.

5.4 Effect of bending stiffness on the free vibration characteristics of a sling network with different vibration absorber positions

For a vibration absorber stiffness of 10^7 N/m, the position of the vibration absorber was changed such that it was located at *L*/3, *L*/4, and *L*/8 from the anchor head of the sling. The natural frequencies *f'* in the C12L (42.048 m) network when not considering the sling's bending stiffness and the natural frequencies *f* in the same network when considering the entire sling's bending stiffness were as given in Table 7 and Fig. 27. The shape of the first 10 modes of the sling network system under different positions of the vibration absorber are shown in Fig. 28.

When the vibration absorber was located at L/3 on the sling, with the exception of the order in which the mode changed, when considering the entire sling's bending stiffness, the first 20 natural frequencies were up to 7.18 % higher than those when the sling's bending stiffness was not considered. In the first 10 modes, when the sling's bending stiffness was not considered, the 1st, 3rd, 7th, 9th orders were in-phase global

Table 7. Frequency comparison of the first 10 orders of the two-sling system under different positions of the vibration absorber (Hz).

Order	Without considering the bending stiffness			Considering the bending stiffness					
	L/3	L/4	L/8	L/3		L/4		L/8	
	f	f	f	f	θ	f	θ	f	θ
1	2.087 (a)	2.087 (a)	2.087 (a)	2.126 (a)	0.042	2.126 (a)	0.132	2.126 (a)	0.372
2	3.125 (c)	2.779 (c)	2.382 (c)	3.192 (c)	0.562	2.832 (c)	0.566	2.421 (c)	0.571
3	4.174 (a)	4.174 (a)	4.174 (a)	4.258 (a)	0.294	4.258 (a)	0.307	4.258 (a)	0.394
4	6.228 (b)	5.557 (c)	4.764 (c)	6.387 (b)	0.415	5.674 (c)	0.560	4.849 (c)	0.571
5	6.261 (2)	6.261 (a)	6.261 (a)	6.399 (a)	0.228	6.399 (a)	0.385	6.399 (a)	0.422
6	6.261 (1)	8.296 (b)	7.146 (c)	6.537 (b)	0.383	8.527 (b)	0.493	7.292 (c)	0.570
7	8.349 (a)	8.349 (2)	8.349 (a)	8.555 (a)	0.167	8.555 (a)	0.336	8.555 (a)	0.458
8	9.375 (c)	8.349 (1)	9.528 (c)	9.644 (c)	0.552	8.843 (b)	0.405	9.756 (c)	0.568
9	10.436 (a)	10.436 (a)	10.436 (a)	10.731 (a)	0.238	10.731 (a)	0.282	10.731 (a)	0.490
10	12.456 (b)	11.114 (c)	11.910 (c)	12.906 (b)	0.413	11.444 (c)	0.544	12.249 (c)	0.564

(a) is the in-phase global vibration; (b) is the out-of-phase global vibration; (c) is the local vibration of the upper part; (i) is the single vibration of the i-th sling

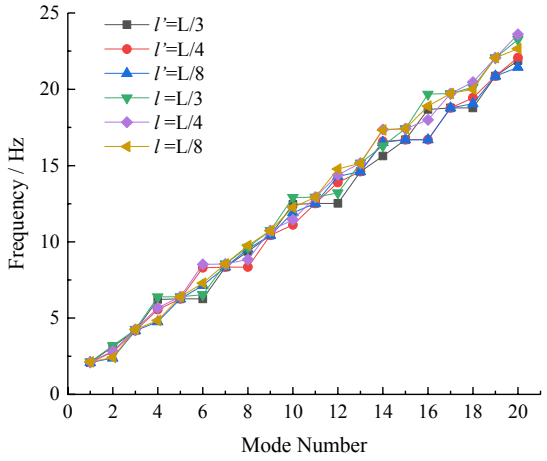

Fig. 27. Curve of the first 20 natural frequencies of the sling network depending on the position of the vibration absorber.

vibration modes, the 4th and 10th orders were out-of-phase global vibration modes, the 2nd and 8th orders were local vibration modes of the upper part, and the 5th and 6th orders were individual vibration modes of a single sling. When considering the entire sling's bending stiffness, with the exception of the 5th order, which changed to in-phase global vibration modes, and the 6th order, which changed to out-of-phase global vibration modes, the vibration modes of the other orders were the same as those without considering the sling's bending stiffness.

When the vibration absorber was located at L/4 on the sling, with the exception of the order in which the mode changed, when considering the entire sling's bending stiffness, the first 20 natural frequencies were up to 6.89 % higher than those when the sling's bending stiffness was not considered. In the first 10 modes, when the sling's bending stiffness was not considered, the 1st, 3rd, 5th, and 9th orders were in-phase global vibration modes, the 6th order was an out-of-phase global vibration mode, the 2nd, 4th, and 10th orders were local vibration modes of the upper part, and the 7th and 8th orders were individual vibration modes of a single sling. When considering the entire sling's bending stiffness, with the exception of the 7th order, which changed to in-phase global vibration modes, and the 8th order, which changed to out-of-phase global vibration modes, the vibration modes of the orders were the same as those without considering the sling's bending stiffness.

When the vibration absorber was located at L/8 on the sling, with the exception of the order in which the mode changed, when considering the entire sling's bending stiffness, the first 20 natural frequencies were up to 5.73 % higher than those when the sling's bending stiffness was not considered. In the first 10 modes, when the sling's bending stiffness was not considered, the 1st, 3rd, 5th, 7th, and 9th orders were in-phase global vibration modes, and the 2nd, 4th, 6th, 8th, and 10th orders were local vibration modes of the upper part. When considering the entire sling's bending stiffness, the vibration modes of the remaining orders were the same as those without considering the sling's bending stiffness.

Thus, for a system with two slings and a single vibration absorber, in the case where the position of the vibration absorber is the same, the frequency of the network system will increase as the cable's bending stiffness increases. When the sling's bending stiffness was not considered and the vibration absorber was located at L/n on the sling, with the exception of when the vibration absorber was in the middle of the sling, every (2*n*) order was one period of change. The (2*n*-1) order and the (2*n*) order in a given period were individual vibration modes of a single sling, the remainder of the odd orders in a given period were the in-phase global vibration modes, the (2*n*-2) order in a given period was the out-of-phase global vibration mode, and the remainder of the even orders in a given period were the local vibration modes of the upper part. When considering the entire sling's bending stiffness, the mode of the individual vibrations of a single sling will not appear. In every pe-

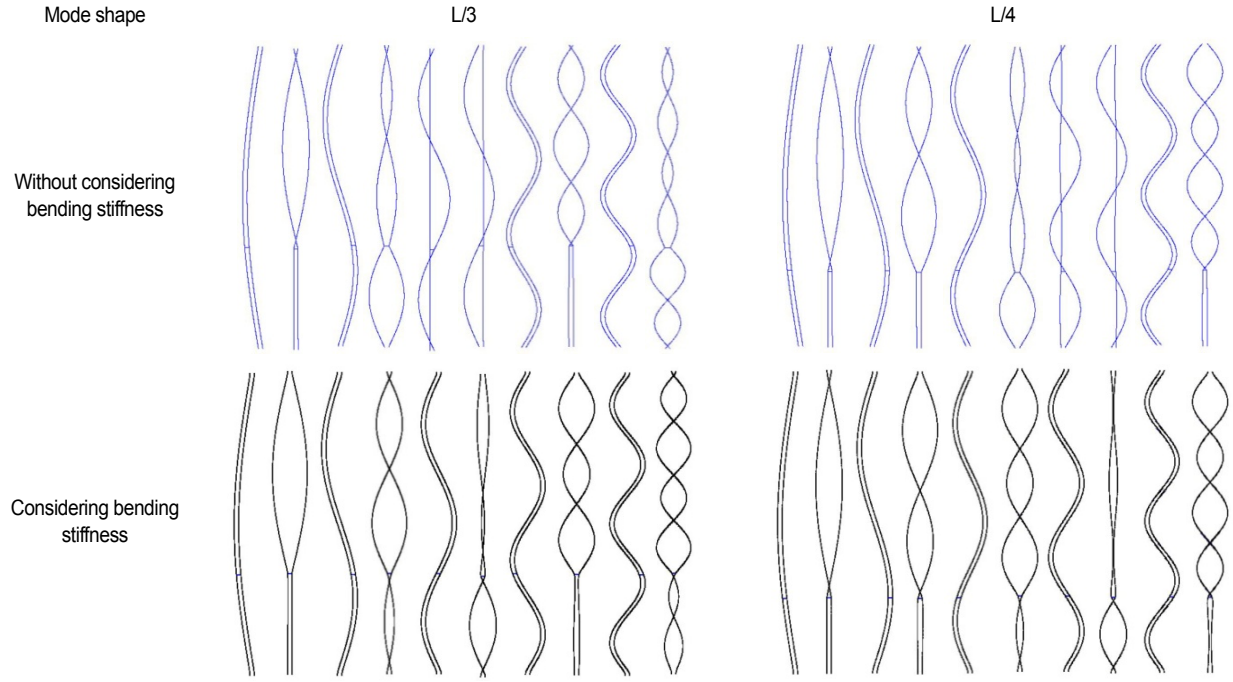

Fig. 28. Shape of the first 10 modes of the system with two slings and a single vibration absorber under different positions of the vibration absorber.

riod, with the exception of the (2*n*-1) order, which changed to in-phase global vibration modes, and the (2*n*) order, which changed to out-of-phase global vibration modes, the vibration modes of the orders were the same as those when not considering the sling's bending stiffness. When the mode was an in-phase global vibration mode or an out-of-phase global vibration mode, $\theta \leq 0.5$, and when the mode was a local vibration mode, $\theta > 0.5$. As the vibration absorber approaches the anchorage point, the increasing percentage of the frequencies when considering the bending stiffness decreases compared with those without considering the bending stiffness so that the effect of the bending stiffness on the frequency of the cable network system decreases. In addition, in the case where the sling's bending stiffness is the same, the frequency and the mode of the in-phase global mode will not change with the position of the vibration absorber, whereas the frequency and mode of the out-of-phase global mode and the local vibration mode of the upper part will be affected by the position of the vibration absorber. The frequency of the local vibration mode of the upper part decreases as the vibration absorber approaches the anchorage point.

5.5 Effect of bending stiffness on the free vibration characteristics of a sling network with different number of vibration absorbers

When the vibration absorber stiffness is 10^7 N/m, by changing the number of vibration absorbers, the number of vibration absorber is 2, 3, or 4. The distance of each vibration absorber is L/(n+1) on the sling. The natural frequencies *f'* in the C12L (42.048 m) network, while not considering the sling's bending stiffness and the natural frequencies *f* in the C12L (42.048 m) network, while considering the entire sling's bending stiffness, are as shown in Table 8 and Fig. 29.

When the number of vibration absorbers was 2, when considering the entire sling's bending stiffness, the first 20 natural frequencies were up to 7.72 % higher than those when the sling's bending stiffness was not considered. In the first 10 modes, when the sling's bending stiffness was not considered, the 1st, 2nd, 7th, and 8th orders were in-phase global vibration modes; the 3rd, 4th, 9th, and 10th orders were out-of-phase global vibration modes; and the 5th and 6th orders were individual vibration modes of a single sling. When considering the entire sling's bending stiffness, the 1st, 2nd, 4th, 7th, 8th, and 10th orders were in-phase global vibration modes and the 3rd, 5th, 6th, and 9th orders were out-of-phase global vibration modes; there were no individual vibration modes of a single sling.

When the number of vibration absorbers was 3, when considering the entire sling's bending stiffness, the first 20 natural frequencies were up to 8.56 % higher than those when the sling's bending stiffness was not considered. In the first 10 modes, when the sling's bending stiffness was not considered, the 1st, 2nd, 3rd, 9th, and 10th orders were in-phase global vibration modes; the 4th, 5th, and 6th orders were out-of-phase global vibration modes; and the 7th and 8th orders were individual vibration modes of a single sling. When considering the entire sling's bending stiffness, the 1st, 2nd, 3rd, 5th, 9th, and 10th orders were in-phase global vibration modes and the 4th, 6th, 7th, and 8th orders were out-of-phase global vibration modes; there were no individual vibration modes of a single sling.

When the number of vibration absorbers was 4, when con-

Table 8. Frequency comparison of the first 10 orders of the two-sling system under different numbers of vibration absorbers (Hz).

Order	Without considering the bending stiffness			Considering the bending stiffness		
	Two vibration absorbers	Three vibration absorbers	Four vibration absorbers	Two vibration absorbers	Three vibration absorbers	Four vibration absorbers
1	2.087 (a)	2.087 (a)	2.087 (a)	2.126 (a)	2.126 (a)	2.126 (a)
2	4.174 (a)	4.174 (a)	4.174 (a)	4.258 (a)	4.258 (a)	4.258 (a)
3	6.195 (b)	6.261 (a)	6.261 (a)	6.360 (b)	6.399 (a)	6.399 (a)
4	6.239 (b)	8.215 (b)	8.349 (a)	6.399 (a)	8.477 (b)	8.555 (a)
5	6.261 (2)	8.270 (b)	10.216 (b)	6.521 (b)	8.555 (a)	10.613 (b)
6	6.261 (1)	8.325 (b)	10.276 (b)	6.573 (b)	8.659 (b)	10.731 (a)
7	8.349 (a)	8.349 (2)	10.351 (b)	8.555 (a)	8.866 (b)	10.807 (b)
8	10.436 (a)	8.349 (1)	10.412 (b)	10.731 (a)	8.910 (b)	11.056 (b)
9	12.390 (b)	10.436 (a)	10.436 (2)	12.852 (b)	10.731 (a)	11.298 (b)
10	12.478 (b)	12.523 (a)	10.436 (1)	12.931 (a)	12.931 (a)	11.333 (b)

(a) is the in-phase global vibration; (b) is the out-of-phase global vibration; (i) is the single vibration of the i-th sling

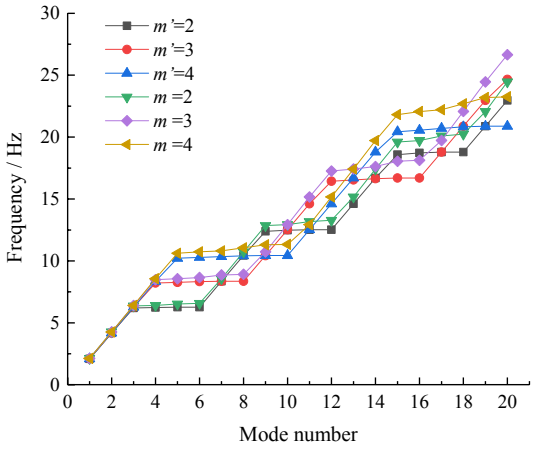

Fig. 29. Curve of the first 20 natural frequencies of the sling network depending on the number of vibration absorbers.

sidering the entire sling's bending stiffness, the first 20 natural frequencies were up to 11.40 % higher than those when the sling's bending stiffness was not considered. In the first 10 modes, when the sling's bending stiffness was not considered, the 1st, 2nd, 3rd, and 4th orders were in-phase global vibration modes; the 5th, 6th, 7th, and 8th orders were out-of-phase global vibration modes; and the 9th and 10th orders were individual vibration modes of a single sling. When considering the entire sling's bending stiffness, the 1st, 2nd, 3rd, 4th, and 6th orders were in-phase global vibration modes and the 5th, 7th, 8th, 9th, and 10th orders were out-of-phase global vibration modes; there were no individual vibration modes of a single sling.

Thus, for a system with two slings, in the case where the number of vibration absorbers is the same, the frequency of the network system will increase as the cable's bending stiffness increases. When the sling's bending stiffness is not considered and the number of vibration absorbers is located at n, every 2(n+1) order is one period of change. The first 1 to n orders in a given period are the in-phase global vibration modes. Meanwhile, the frequency of the in-phase global vibrations does not change with the change in the number of vibration absorbers. The orders n+1 to 2n in a given period are the out-of-phase global vibration modes, while the orders 2n+1 to 2n+2 in a given period are the modes of the individual vibrations of a single sling. When considering the entire sling's bending stiffness, every 2(n+1) order is still one period but the mode of the individual vibrations of a single sling will not appear. The first 1 to n orders and the (n+2) order in a given period are the in-phase global vibration modes, and the remaining orders in a given period are the out-of-phase global vibration modes. As the number of vibration absorbers increases, when considering the bending stiffness, the increasing percentage of the frequencies also increases in relation to those without considering the bending stiffness, such that the effect of bending stiffness on the frequencies of the cable network system increases. In addition, in the case where the sling's bending stiffness is the same, when the number of vibration absorbers is changed, the fundamental frequency of the sling network structure and the frequency of the in-phase global vibration do not change. However, the higher the number of vibration absorbers, the later the mode of the out-of-phase global vibration will occur, and the larger the minimum frequency of the out-of-phase global vibration will be.

6. Conclusions

The results from theoretical derivations and parameter analysis research on the influence of the bending stiffness on the in-plane free vibration characteristics of a cable network system can be concluded as follows:

1) After considering the cable's bending stiffness, the cable network's natural frequency clearly increases. Moreover, the slings network's increase in amplitude is larger than that of the stay-cable network, and the influence of the sling's bending stiffness is more obvious. After the cable network system is

formed by the cross-ties or the vibration absorber, each cable's natural frequency is the same, and the local vibration frequency, or the individual vibration frequency of a single cable, occurs between the global vibration frequencies.

2) For the multilayer unequal-length stay-cable network, the application of cross-ties increases the target cable's fundamental frequency. As the cable's bending stiffness increases, the frequency of the network system will increase, and the orders of a part of modes will slightly change but the shapes do not change. If the cross-tie is at the middle of the cable, there are local vibration modes for multiple cables as well as the individual vibration modes of single cable between the global vibration modes. However, when the cross-tie is at a position other than at the middle of the cable, the individual vibration modes of a single cable do not appear. The global vibration frequencies and local vibration frequencies of multiple cables will decrease as the cross-tie stiffness decreases, but a single cable's individual vibration frequencies do not change as the cross-tie stiffness changes. Besides, as the cross-tie stiffness decreases, the increasing percentage of the frequencies when considering the bending stiffness and those frequencies without considering the bending stiffness also decreases. Except when the cross-tie is located at $L/2$ on the target cable, as the position of the cross-tie approaches the anchor point, the increasing percentage of the frequencies when considering the bending stiffness increases compared with those without considering the bending stiffness. The effect of the cross-ties position on the cable network's fundamental frequency is not obvious.

3) As the number of cross-ties increases, the fundamental frequency of the five-cable system increases accordingly, and the later the local vibration mode shape appears, the larger the minimum frequency of local vibration occurs. Besides, as the number of cross-ties increases, the influence of the cable's bending stiffness is more obvious. As the number of cables decreases, the cable network's fundamental frequency decreases. There are (n–1) local vibration modes between the global vibration modes in the n cable system. Besides, the influence of the cable's bending stiffness is less obvious as the number of cables decreases.

4) For the double-layer equal-length sling network, the fundamental frequency of the sling network structure does not change when applying the vibration absorber. As the sling's bending stiffness increases, the frequency of the network system will increase and the orders and shapes of a part of the modes will change. The nondimensional index θ can be used to assess the degree of mode localization. There are individual vibration modes of a single sling (appearing in pairs when the vibration absorber is locate at the middle of sling) as well as out-of-phase vibration modes between the in-phase global vibration modes. The shorter the sling length, the more obvious is the influence of bending stiffness. As the stiffness of the vibration absorber decreases, the frequency of the in-phase global vibrations and the individual vibrations of a single sling remain unchanged, while the frequency of the out-of-phase global vibrations decreases. Besides, when the vibration absorber stiffness is more than 10^6 N/m, a "jump phenomenon of order" will appear when considering the sling's bending stiffness. As the vibration absorber stiffness decreases, the increasing percentage of the frequencies when considering the bending stiffness and those frequencies without considering the bending stiffness also decreases.

5) As the vibration absorber approaches the anchorage point, the increasing percentage of the frequencies when considering the bending stiffness decreases compared with those without considering the bending stiffness. The frequency and mode of the in-phase global mode will not change with the position of the vibration absorber; however, the frequency and mode of the out-of-phase global mode and the local vibration mode of the upper part are affected by the position of the vibration absorber. As the number of vibration absorbers increases, the sling network's fundamental frequency and the frequency of the in-phase global vibration do not change, while the later that the mode of the out-of-phase global vibrations occurs, the larger the minimum frequency of the out-of-phase global vibration appears. The greater the number of vibration absorbers, the more obvious is the influence of the bending stiffness.

Acknowledgments

This work was supported by the National Natural Science Foundation of China (51678247,51908382), the Natural Science Foundation of Hebei Province (E2019210311), and Research project of the State Key Laboratory of Mechanical Behavior and System Safety of Traffic Engineering Structures (ZZ2020-21), China.

References

[1] E. Laursen, N. Bitsch and J. E. Andersen, Analysis and mitigation of large amplitude cable vibrations at the great belt east bridge, *IABSE Symposium Report. International Association for Bridge and Structural Engineering*, 91 (3) (2006) 64-71.

[2] S. H. Cheng, P. A. Irwin and H. Tanaka, Experimental study on the wind-induced vibration of a dry inclined cable-Part II: proposed mechanism, *Journal of Wind Engineering and Industrial Aerodynamics*, 96 (12) (2008) 2254-2272.

[3] X. Wang, Wind tunnel test on galloping of iced conductors and galloping simulation for transmission tower-line system, *Ph.D. Thesis*, Zhejiang University, Hangzhou, China (2011).

[4] H. M. Irvine, *Cable Structures*, The MIT Press, Cambridge (1981).

[5] H. Zui, T. Shinke and Y. Namita, Practical formulas for estimation of cable tension by vibration method, *Journal of Structural Engineering*, 122 (6) (1996) 651-656.

[6] A. B. Mehrabi and H. Tabatabai, Unified finite difference formulation for free vibration of cables, *Journal of Structural Engineering*, 124 (11) (1998) 1313-1322.

[7] Y. H. Huang, J. Y. Fu and R. H. Wang, Practical formula to calculate tension of vertical cable with hinged-fixed conditions based on vibration method, *Journal of Vibroengineering*, 16 (2)

(2014) 997-1009.
[8] H. Z. Xu and P. M. Huang, Test and research on cable force with damping frames, *Highway*, 2003 (8) 76-79.
[9] T. B. Li, Y. J. Dai and R. X. Ren, Testing research on the cable force with vibration damper, *Shanxi Architecture*, 35 (16) (2009) 331-332.
[10] Q. Gan, Estimation method of tension in cables under complex boundary conditions, *Ph.D. Thesis*, South China University of Technology, Guangzhou, China (2015).
[11] P. J. Li, Research on vibration parameters identification of cable-strut with multi-support, *Ph.D. Thesis*, South China University of Technology, Guangzhou, China (2012).
[12] P. L. Verniere, G. M. Ficcadenti and P. A. A. Laura, Dynamic analysis of a beam with an intermediate elastic support, *Journal of Sound and Vibration*, 96 (3) (1984) 381-389.
[13] H. Xu and W. L. Li, Dynamic behavior of multi-span bridges under moving loads with focusing on the effect of the coupling conditions between spans, *Journal of Sound and Vibration*, 312 (4-5) (2008) 736-753.
[14] H. Y. Lin, Dynamic analysis of a multi-span uniform beam carrying a number of various concentrated elements, *Journal of Sound and Vibration*, 309 (1-2) (2008) 262-275.
[15] X. Wu, Natural transversal vibrating frequency of continuous long cable with multi-spans, *Journal of Vibration and Shock*, 24 (4) (2005) 127-129.
[16] D. Shu and C. N. Della, Free vibration analysis of composite beams with two non-overlapping delaminations, *International Journal of Mechanical Sciences*, 46 (4) (2004) 209-526.
[17] C. N. Della, D. Shu and P. Msrao, Vibrations of beams with two overlappig delaminations, *Composite Structures*, 66 (1-4) (2004) 101-108.
[18] L. Caracoglia and N. P. Jones, In-plane dynamic behavior of cable networks: part1: formulation and basic solutions, *Journal of Sound and Vibration*, 279 (3) (2005) 969-991.
[19] L. Caracoglia and N. P. Jones, In-plane dynamic behavior of cable networks: part 2: prototype prediction and validation, *Journal of Sound and Vibration*, 279 (3) (2005) 993-1014.
[20] J. Ahmad, S. H. Cheng and F. Z. Ghrib, Impact of cross-tie design on the in-plane stiffness and local mode formation of cable networks on cable-stayed bridges, *Journal of Sound and Vibration*, 363 (2016) 141-155.
[21] J. Ahmad, In-plane dynamic behaviour of conventional and hybrid cable network systems on cable-stayed bridges, *Ph.D. Thesis*, University of Windsor, Windsor, Canada (2016).
[22] J. Ahmad, Combined effect of external damper and cross-tie on the modal response of hybrid two networks, *Journal of Sound and Vibration*, 417 (2018) 132-148.
[23] H. Yamaguchi, Control of cable vibrations with secondary cables, *Proceedings of the International Symposium on Cable*, *Dynamics* (1995) 445-452.
[24] H. J. Zhou, X. B. Zhou and G. Z. Yao, Free vibration of two taut cables interconnected by a damper, *Structural Control and Health Monitoring*, 26 (10) (2019) e2423.
[25] H. J. Zhou, X. Yang and Y. R. Peng, Damping and frequency of twin-cables with a cross-link and a viscous damper, *Smart Structures and Systems*, 23 (6) (2019) 669-682.
[26] H. J. Zhou, X. Yang and L. M. Sun, Free vibrations of a two-cable network with near-support dampers and a cross-link, *Structural Control and Health Monitoring*, 22 (9) (2015) 1173-1192.
[27] H. J. Zhou, Y. H. Wu and L. X. Li, Free vibrations of a two-cable network inter-supported by cross-links extended to ground, *Smart Structures and Systems*, 23 (6) (2019) 653-667.
[28] H. J. Zhou, S. K. Qi and G. Z. Yao, Damping and frequency of a model cable attached with a pre-tensioned shape memory alloy wire: experiment and analysis, *Structural Control & Health Monitoring*, 25 (2) (2018) 1-19.
[29] H. J. Zhou, L. M. Sun and F. Xing, Free vibration of taut cable with a damper and a spring, *Structural Control Health Monitoring*, 21 (6) (2014) 996-1014.
[30] L. M. Sun, Y. G. Zhou and H. W. Huang, Experiment and damping evaluation on stay cables connected by cross ties, *Proceedings of 7th International Symposium on Cable Dynamics*, Vienna (2007) 175-182.
[31] Y. G. Zhou, Dynamic characteristics and vibration mitigation of stay cables using cross ties, *Ph.D. Thesis*, Tongji University, Shanghai, Chian (2007).
[32] J. M. Huang, Study on vibration reduction of cross ties in long-span cable-tayed bridges, *Proceedings of 2000 Annual Conference of Municipal Engineering Branch of Chinese Society of Civil Engineering* (2000) 374-385.
[33] Z. Q. Chen, X. Lei and X. G. Hua, Research and application of vibration control method for sling cables in long-span suspension Bridge, *Journal of Hunan University (Natural Sciences)*, 43 (1) (2016) 1-10.
[34] X. Lei, Study about wind(rain) effects and vibration control of flexible structural members in long-span bridge, *Ph.D. Thesis*, Hunan University, Changsha, China (2016).
[35] H. M. Irvine, The linear theory of free vibrations of suspended membranes, *Proceedings of the Royal Society of London*, 350 (1662) (1976) 317-334.
[36] X. M. Wang, Y. Q. Li and H. W. Xu, *Structural Analysis Unit and Application with ANSYS*, China Communication Press, China (2011).
[37] X. M. Wang, *Structural Dynamic Analysis and Application with ANSYS*, China Communication Press, China (2014).
[38] W. X. Ren and G. Chen, Practical formulas to determine cable tension by using cable fundamental frequency, *China Civil Engineering Journal*, 38 (11) (2005) 26-31.

Wei Chen is a doctoral candidate pursuing a Ph.D. degree in Bridge and Tunnel Engineering at South China University of Technology, China. He received his bachelor degree in Civil Engineering at South China University of Technology. His current research area is mainly on the dynamics analysis of the cable network using analytical method.

Xiaoxia Zhen is an Associate Professor of School of Civil Engineering and Transportation, South China University of Technology, China. She received her Ph.D. in Structural Engineering from South China University of Technology. Her current research area is mainly on the structural stability and vibration of the long-span bridge.